INVESTIGATION INTO LINEARITY AND CAUSALITY OF HEMODYNAMIC RESPONSE DURING RESTING STATE

MS Thesis

Muhammad Osama
14060023

Advisor
Dr. Waqas Majeed

Department of Electrical Engineering
Lahore University of Management Sciences

INVESTIGATION INTO LINEARITY AND CAUSALITY OF HEMODYNAMIC RESPONSE DURING RESTING STATE

Muhammad Osama
2014-06-0023

Department of Electrical Engineering

MS Thesis

May 2016

LAHORE UNIVERITY OF MANAGEMENT SCIENCES

Department of Electrical Engineering

CERTIFICATE

I hereby recommend that the thesis prepared under my supervision by:

Muhammad Osama

on title: **INVESTIGATION INTO LINEARITY AND CAUSALITY OF HEMODYNAMIC RESPONSE DURING RESTING STATE**

be accepted in partial fulfillment of the requirements for the MS degree.

Dr. Waqas Majeed
Advisor (Chairperson of Defense Committee)

Recommendation of Thesis Defense Committee:
(at least a Supervisor and one more member is required as per rule)

Dr. Momin Uppal
Name ***Signature*** ***Date***

Dr. Muhammad Tahir
Name ***Signature*** ***Date***

ACKNOWLEDGEMENT

First of all I would thank Almighty Allah because without His help and permission, this thesis, even MS or even my thought process or anything else would not have been possible. I would also thank Allah for providing me Dr. Waqas Majeed as a supervisor. I do not think I could have been supervised by anybody better than Sir Waqas did. Throughout thesis and my tenure as his Research Assistant, Sir Waqas boosted my confidence by appreciating even the smallest of my work which I would feel is nothing special. My knowledge and research skills were enhanced as he showed me new and intuitive ways of looking at problems. I cannot thank him enough. I pray that may Allah bless him with his most precious of blessings.

I would also thank my parents for their support. Allowing your son to live away from you is difficult for all parents but it would have been more difficult for them since it also meant leaving my job. I hope that I am able to meet my parents' expectations and do something special for them in life.

I would also like to acknowledge data contribution for this thesis by colleagues at Emory University [6].

SUMMARY

Neural activity in any region of the brain is followed by increase in concentration of oxygenated hemoglobin in that region. Functional magnetic resonance imaging (fMRI) is sensitive to local changes in concentration of oxyhemoglobin, resulting in blood-oxygen level dependent (BOLD) signal.

It is crucial to quantify the relationship between neural activity and BOLD signal so that correct inferences about neural activity can be made from the non-invasively obtained BOLD signal. A lot of research has been done in this area. For example [1] showed that the system between neural activity and BOLD response from human visual cortex exhibits non-linearity for small inter-stimulus interval (ISI) between paired stimuli. [3] showed that the estimated impulse response of a linear time invariant (LTI) model between stimulus and BOLD response changes with stimulus duration. These conclusions have been made for studies done in a task-based paradigm of fMRI in which the subject is shown some visual stimulus. However, there is growing interest in another paradigm of fMRI called resting-state in which the subject is provided no overt stimulus. This is because it has been observed that the BOLD signal during resting state is not random noise but is specifically organized. Moreover, most of the energy consumed by the brain is associated with neural activity during resting state. In order to make quantitative inferences about the underlying neural activity based on resting-state BOLD activity, it is important to investigate whether the relationship between BOLD and neural activity at resting state can be modeled as a linear system, or whether the results regarding non-linearity between neural activity and BOLD in task-based paradigm hold for the case of resting-state.

Although the relationship between the task-induced BOLD response and task-induced neural activity is strictly causal, a non-causal relationship is plausible between resting state BOLD and neural activity. During resting state, there is no overt stimulus or task to drive the neural activity and change in oxygenation of hemoglobin. However, there are spontaneous fluctuations in the diameter (tone) of blood vessels which are independent of heartbeat, respiration or innervations which is called vasomotion. Although, vasomotion (and hence hemodynamic signal) may precede the neural activity due to some common mechanism controlling vasomotion and resting-state neural activity, this possibility has not been investigated previously. It is even possible that vasomotion itself directly derives the neural activity and hemodynamic signal.

In this study, we have investigated the linearity between neural activity and BOLD signal by using local filed potential (LFP) and optically measured hemodynamic response, acquired in rat brain during resting state and provided to us by colleagues at Emory University [6]. The LFP signal consisted of periods of activity marked by bursts and silent periods of inactivity. We examined whether the observed optical response deviates from the response of an LTI system for small inter-burst-interval (IBI) and whether the estimated impulse response changes as crowdedness of neural activity bursts changes with time. We show that that contrary to the results for task-based setting, there is no evidence of non-linearity between neural activity and optically measured hemodynamic signal in resting state. . We also studied the causality of impulse response and granger-causal influences between neural activity and BOLD using least-square filtering and Granger-causality technique respectively. This study differed from previous studies on causality in that the results were also obtained with the presence of inherent noise in data taken into consideration. It was found that the impulse response between LFP and optical signal during resting state is statistically non-causal (hinting towards the possibility of a third

agent controlling both neural activity and oxygenation) and optical signal also has causal influence on LFP. But it was also found that the presence of noise inherent in data makes the filter estimates obtained by widely used techniques such as least-square filtering and weiner filtering biased and can also lead to false granger-causal influences. This raises questions regarding inferences made about underlying physiological systems in fMRI studies from hemodynamic response functions (HRF) which are obtained using least-square technique. It also raises questions on the granger causal influences reported in studies such as [12] and stresses the need for practicing caution while interpreting results of studies that involve the use of these techniques.

TABLE OF CONTENTS

LIST OF FIGURES

LIST OF TABLES

LIST OF ABBREVIATIONS

Following are the abbreviations and acronyms used in the document:

fMRI	-	Functional Magnetic Resonance Imaging
BOLD	-	Blood Oxygenation Level Dependent
LFP	-	Local Field Potential
HRF	-	Hemodynamic Response Function
ISI	-	Inter-Stimulus Interval
IBI	-	Inter Burst Interval
LTI	-	Linear Time Invariant
SI	-	Somatosensory cortex
MDL	-	Minimum Description Length
RLS	-	Recursive Least Square

1. INTRODUCTION

Functional magnetic resonance imaging (fMRI) has been a revolutionary technique in neuroscience research. It has enabled the study of functional organization of the brain i.e. which brain region activates in response to a particular task. It has been used to study functional and structural connectivity of the brain and the relationship between them i.e. which brain regions work in coherence with one another in response to task. It has been used to find biomarkers for diseases such as schizophrenia and epilepsy by correlating them to higher or lower activation in specific brain regions compared to that of a healthy person. In short fMRI has grown to become an indispensible tool in brain research. It has enhanced our understanding of the underlying cognitive processes in the brain and provides limitless possibilities for further research.

1.1 A BRIEF BACKGROUND OF MRI

fMRI is a non-invasive technique. It is based on the principle of nuclear magnetic resonance and the magnetic state of hemoglobin. Hydrogen nuclei possess a characteristic spin and since they are charged they also have a magnetic moment. In absence of an external magnetic field, the magnetic moments of the different hydrogen nuclei are in random directions. However, when an object is placed in a large magnetic field $\mathbf{B_0}$ (0.5 to 1.5 T) the hydrogen nuclei align with the external magnetic field and precess about it like a gyroscope with a frequency called the Larmor frequency given by $w_0 = \gamma * B_0$. This gives rise to a net magnetic moment **M** in the direction of the external field precessing at larmor frequency. When a radio frequency pulse $\mathbf{B_{rf}}$ whose frequency is equal to $\boldsymbol{w_0}$ is applied perpendicular to $\mathbf{B_0}$ it causes **M** to tilt away from $\mathbf{B_0}$. When $\mathbf{B_{rf}}$ is removed, **M** tends to realign itself with $\mathbf{B_0}$ a process called relaxation. Coils placed around the object being imaged sense the motion of this magnetic moment vector **M** during relaxation

and this constitutes a radio frequency signal. The brain is divided into hundreds of small cubicle elements called voxels. The MRI signal for a given voxel in a T2-weighted image depends on the **B** field inhomogenity.

1.2 THE PHYSIOLOGICAL BASIS OF FMRI

The **B** field inhomogenity in a voxel itself depends on the oxygen concentration of the hemoglobin around the hydrogen nuclei. Deoxygenated hemoglobin is paramagnetic and increases the inhomogenity and tends to reduce the MR signal. When a subject performs some task or is shown some stimulus e.g. a visual checkerboard it results in electrical signals called action potential generated by neurons through their axons. Chemical reactions follow action potential and trigger the release of neurotransmitters from the transmitting neurons (pre-synaptic side) to the receiving neurons (post-synaptic side)Figure 1-1: .

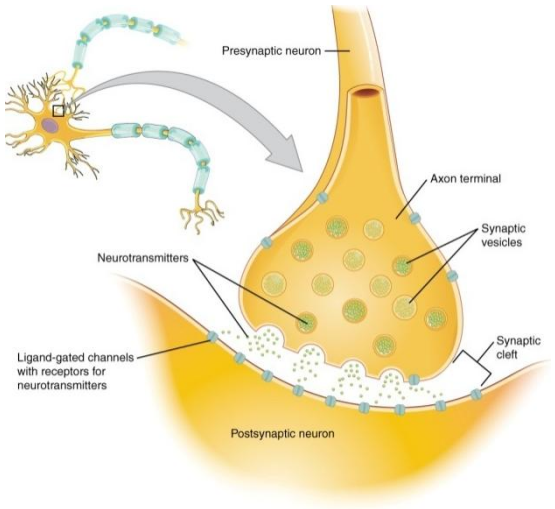

Figure 1-1: Pre-synaptic and post-synaptic side of a neuron

These chemical reactions are downhill and therefore no energy is required, however, the restoration of ionic gradients and recycling of neurotransmitters for the next action potential

requires energy in the form of adenosine triphosphate (ATP). ATP is synthesized by two processes. One is glycolysis which requires glucose and produces small amount of ATP. The other one is oxidative glucose metabolism which requires oxygen and produces large amount of ATP. A constant supply of glucose and oxygen is therefore necessary for cerebral metabolism. The supply of these two energy substrates is maintained by cerebral blood flow (CBF). So following neural activity is an increase in CBF. However, the increase in oxygen consumption is less than CBF so there is a net increase in the concentration of oxygenated hemoglobin. Oxygen extraction fraction (E) which intuitively is a ratio of oxygen consumption to oxygen supply decreases with activation. Since oxygenated hemoglobin is diamagnetic, the increase in blood oxygenation during activation changes the magnetic properties of the blood and tissue and causes the MR signal to increase. This physiological processes that follow increased neural activity are called neuro-vascular coupling or hemodynamic response. This is the basis for the blood-oxygen level dependent (BOLD) signal observed in fMRI. A typical BOLD signal is shown in Figure 1-2 which can be seen to increase when the stimulus is ON.

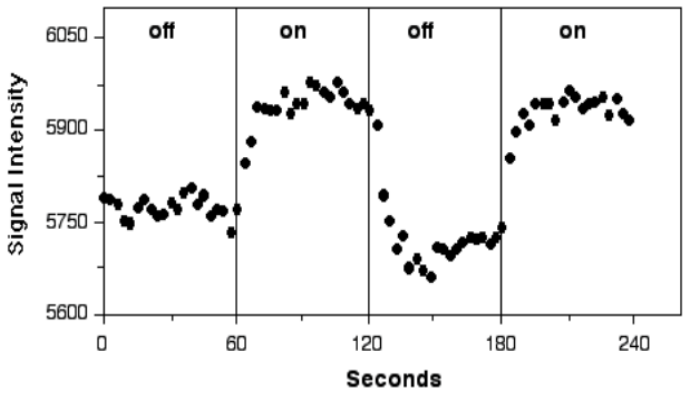

Figure 1-2: A typical BOLD response

1.3 TYPES OF FMRI EXPERIMENTS

fMRI experiments fall into two categories:

1.1.1 Task based

In task-based fMRI experiments, the subject is presented with a stimulus (e.g. a visual checker board) or is asked to perform a task (such as tapping his fingers or closing and opening his eyes) during the acquisition of fMRI data. Most task-based fMRI experiments utilize a block-design paradigm: There are ON-OFF blocks of stimulus i.e. there are periods during which the stimulus in ON followed by periods during which the stimulus is OFF and ON again. The brain is divided into thousands of tiny cubical elements called voxels and as the stimulus is turned ON and OFF, the BOLD signal from different voxels of the brain is also measured. Then generalized linear model is fit between the BOLD signal and the stimulus/task to detect the voxels for which the BOLD signal is significantly influenced by the stimulus/task, and hence find out which brain regions activated in response to the task or stimulus allowing us to relate function to its responsible brain region.

1.1.2 Resting-state

Resting state is the other important paradigm in fMRI studies. In these experiments the subject neither performs any task nor is he shown any stimulus during data acquisition. Low frequency BOLD fluctuations have been observed during resting state [4]. It has also been observed that the BOLD signal during resting state is not random noise but is specifically organized. For example, correlation maps of resting state BOLD signals show the presence of a Default Mode Network (DMN) in the brain which is not present when subject is performing some task [15] . Moreover, most of the energy consumed by the brain is associated with neural activity during resting state. In fact the human brain consumes 20% of the body's energy and task-related energy increases

are less than 5% [4]. Furthermore, it has been shown that patients with mild cognitive impairments and mild Alzheimer disease have altered resting state functional connectivity in the default mode network [7] and therefore such alterations could act as an early stage biomarker for cognitive impairments. In short, resting state fMRI has become an important area of research and promises to provide us a deeper understanding of the working of brain.

1.4 MODELING HEMODYNAMIC RESPONSE

There has been a lot of interest in studying the relationship between neural activity and the corresponding BOLD signal. For example [2] showed that the BOLD activity and local field potential (LFP) recordings, which is a representative of the collective/average electrical activity of a group of neurons in a brain region, taken from visual cortex of monkey are highly correlated. [3] investigated the linearity of relationship between BOLD signal from human visual cortex with the duration of visual stimulus. They verified the superposition principle by using responses to stimuli of short duration to predict the response to longer stimuli duration and compared it to the actual response. As shown in Figure 1-3, the RMS error is larger for stimuli of shorter duration. They used this evidence to conclude that at shorter stimuli duration the relationship between stimuli and BOLD is non-linear. They also investigated non-linearity by assuming a linear convolution model and then estimating the impulse response (called the hemodynamic response function) for stimuli of different duration. As can be seen in Figure 1-4 for longer stimuli duration the area under the estimated impulse responses in approximately same but there is a lot of difference for smaller stimuli duration.

[1] investigated whether the non-linearity between stimulus and BOLD was due to the system between stimulus and neural activity or the system between neural activity and BOLD. Using a finding from [8] in which it was shown that for paired stimuli separated by inter-stimulus

interval (ISI) greater than 800ms the system between stimuli and neural activity behaves linearly, they examined the BOLD responses to paired stimuli having different ISIs but all greater than the above threshold. The source of any non-linearity observed now must be the system between neural activity and BOLD. In this paper, the authors compared the BOLD response to a single stimuli to a response obtained after subtracting the single stimuli response from the response of paired stimuli for different ISIs. The subtracted response would be expected to be the same as the response due to single stimuli if the system were linear. But as shown in Figure 1-5 for shorter ISIs the subtracted response has a smaller peak value than the single stimuli response. This shows that for short ISIs there is some kind of saturation/non-linearity in the BOLD response.

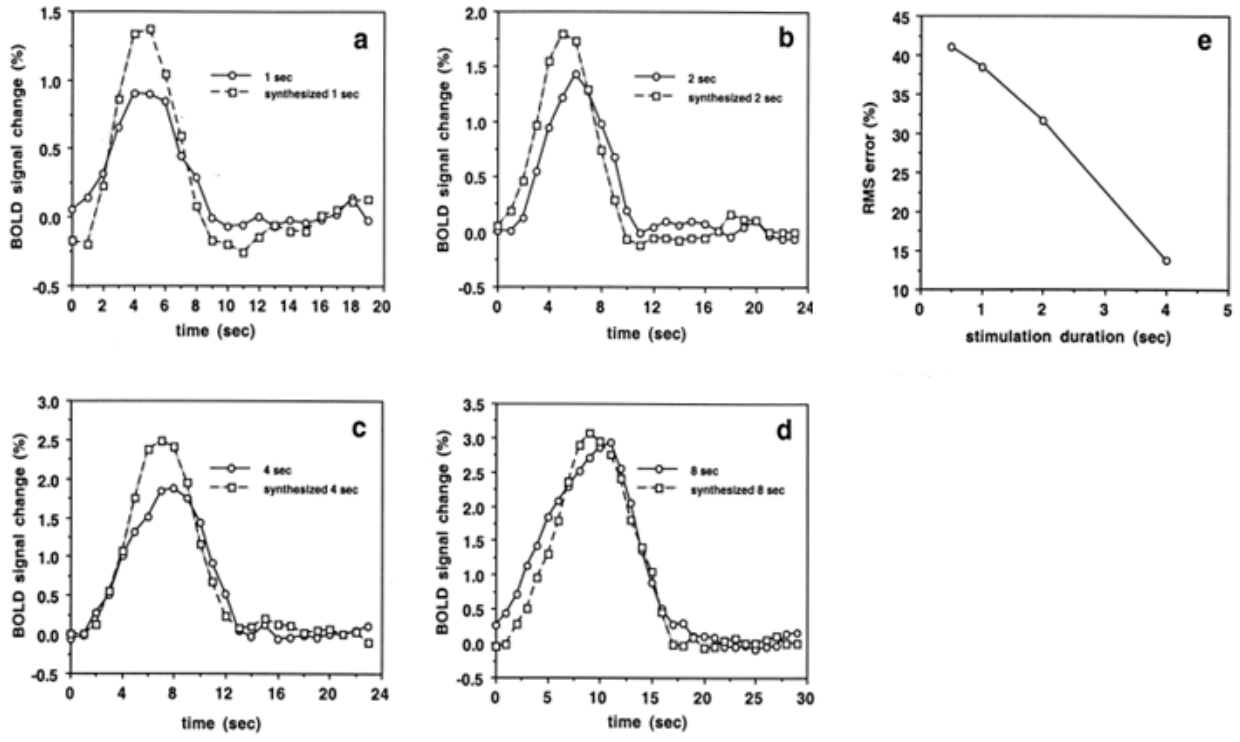

Figure 1-3: Taken from [3] a) True vs. synthesized BOLD signal for stimulus duration of 1 sec b) True vs. synthesized BOLD signal for stimulus duration of 2 sec c) True vs. synthesized BOLD signal for stimulus duration of 4 sec d) True vs. synthesized BOLD signal for stimulus duration of 8 sec e) RMS error b/w true and synthesized BOLD signal for different stimuli durations

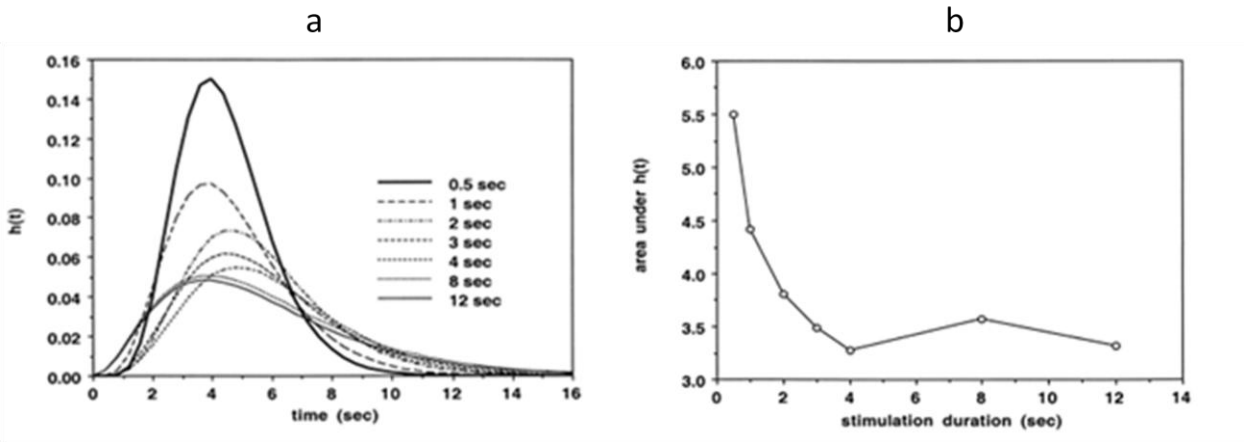

Figure 1-4: Taken from [3] a) The estimated impulse response functions for stimuli of different duration b) the area under the estimated impulse response functions vs. stimuli duration

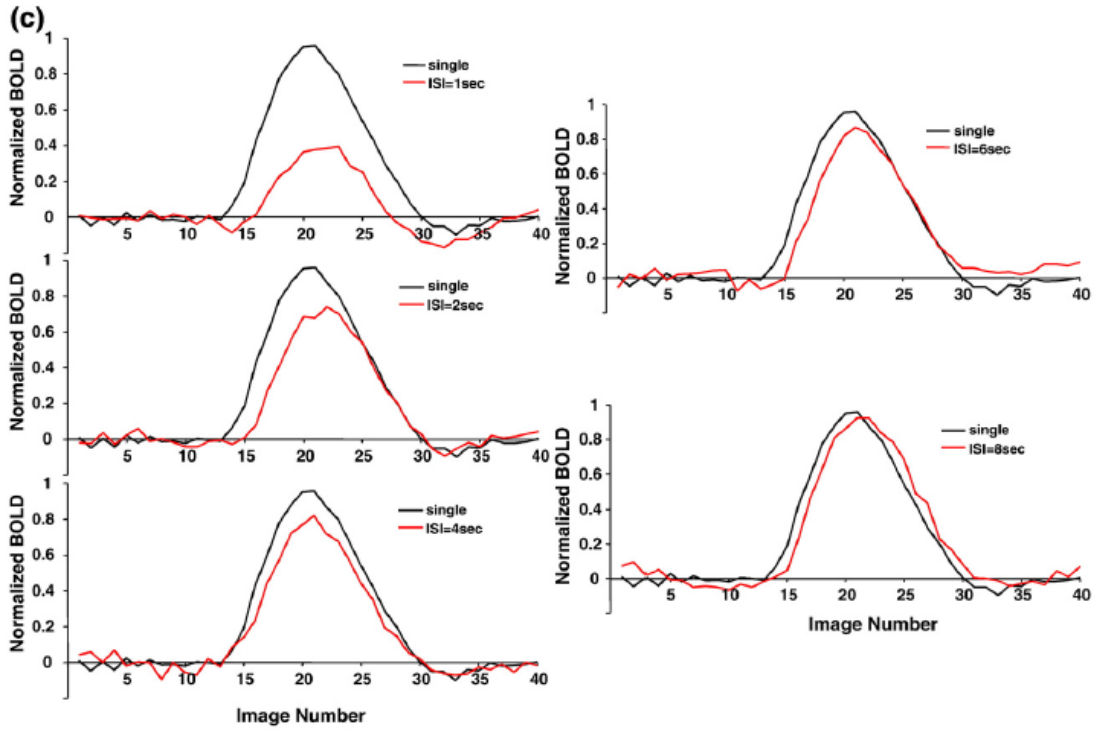

Figure 1-5: Taken from [1] Difference between BOLD response of single stimlus and the subtracted BOLD response obtained by subtracting from BOLD response due to paired stimuli BOLD response to single stimulus for different inter-stimulus interval ISI

1.5 MOTIVATION

All the literature discussed in the previous section studied the relationship between neural activity/stimulus and BOLD in a task-based setting. Given its importance and potential, it would be interesting and enlightening to study the relationship between neural activity and BOLD during resting state. It would be interesting to see whether the conclusions regarding non-linearity between neural activity and BOLD made in case of task based studies hold for resting state as well. There are many unanswered questions. Does BOLD signal during resting state also show non-linearity for small inter-burst interval (IBI) in neural activity? Is the impulse response different under different condition of input e.g. when neural activity bursts occur close and when they are far? Does two times BOLD imply two times neural activity in resting state? Secondly, neural activity and BOLD response during resting state are not caused by any overt task. There is possibility that these signals are driven by vasomotion which is the spontaneous fluctuation of tone of blood vessels independent of heartbeat or respiration. Therefore it would be interesting to address such possibility by studying the causality of impulse response between neural activity and BOLD and investigating causal influences between the two signals. Simultaneous BOLD-LFP recordings can help us study this relationship, however, LFP recordings taken together during fMRI are corrupted by artifacts such as gradient artifacts. Fortunately, hemodynamic response to neural activity can be measured using an optical approach. Our colleagues at Emory University have shared with us simultaneous recordings of LFP and the surrogate BOLD signal (which we call the optical signal) of rat brain during resting-state which we have used to address the above questions.

2. DATA DESCRIPTION AND PRE-PROCESSING

The data used in this work was provided to us by colleagues at Emory University [6] The data set consist of simultaneous hemodynamic and local field potential (LFP) recordings from the primary somatosensory cortex (S1) region of Sprague-Dawley rats obtained at 1200Hz sampling rate by the method of functional near infrared spectroscopy (NIRS). The rats were under 1.8 % isoflurane during 7min recording session. In NIRS two fine optical fibers were placed adjacent to one another for light delivery and photon detection at the same site and connected to an LED light source of (660nm, 810nm or 940nm) and photodiode detector. Micro-gas electrodes were used for the measurement of LFP recordings. For the measurement of hemodynamic recordings, the method relies on the infrared absorption property of oxygenated hemoglobin. Neuronal activity in a brain region is followed by increased cerebral blood flow and increase in the concentration of oxygenated hemoglobin resulting in greater absorption of the infrared being delivered at that site by the optical fiber. As a result there is decrease in the infrared sensed by the photodiode detector and dip is observed in the hemodynamic recording (Figure 2.1b). A raw LFP signal and hemodynamic recording (which we call the optical signal) is shown in Figure 2.1.

2.1 PREPROCESSING PIPELINE

The preprocessing pipeline consist of four steps shown below.

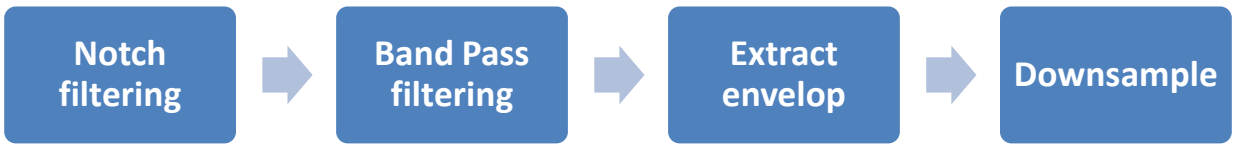

2.1.1 Notch filtering

The data were corrupted by physiological noise i.e. respiratory and cardiac noise. The rate of respiration and cardiac cycle were measured along with data acquisition. The frequencies of the peaks were identified by looking at the power spectrum of the LFP and optically measured hemodynamic signal (Figure 2.1c). Notch filtering with notches located at the fundamental and harmonic frequencies of the cardiac (Figure2.1d) and respiratory cycle were used to filter both the optical signal and the LFP recordings.

2.1.2 Band-pass filtering and envelop extraction

The dips in the optical signal correspond to the presence of neuronal activity and it occurs only when a neuronal activity bursts occurs in the LFP recording (Figure 2.1a). We were only interested in the relationship between LFP bursts and changes in hemodynamic signal because the LFP bursts represents the action potential and release of neuro-transmitters by neurons and we are interested in relating this to the resulting change in oxygenation concentration in hemoglobin.

We eliminated other components in the LFP signal by band-pass filtering the LFP signal from 1 to 50Hz frequency range. This range was chosen empirically by observing which frequency band contained the LFP bursts and in which frequency band the bursts were absent. Moreover, in our study we were interested in finding out a relationship between the synaptic activity of neurons and the hemodynamic signal. A burst observed in the LFP recording corresponds to high synaptic activity and the absence of burst corresponds to low or zero synaptic activity. Therefore the synaptic activity could be estimated by the envelope of LFP recordings. Hilbert transform was used to extract the envelope Figure 2.1e).

2.1.3 Downsampling

At this stage, both the LFP envelope and the optical signal were low frequency signals with a maximum frequency less than 5Hz. Therefore as a final pre-processing step the signals were down-sampled from a sampling frequency of 1200Hz to 10Hz.

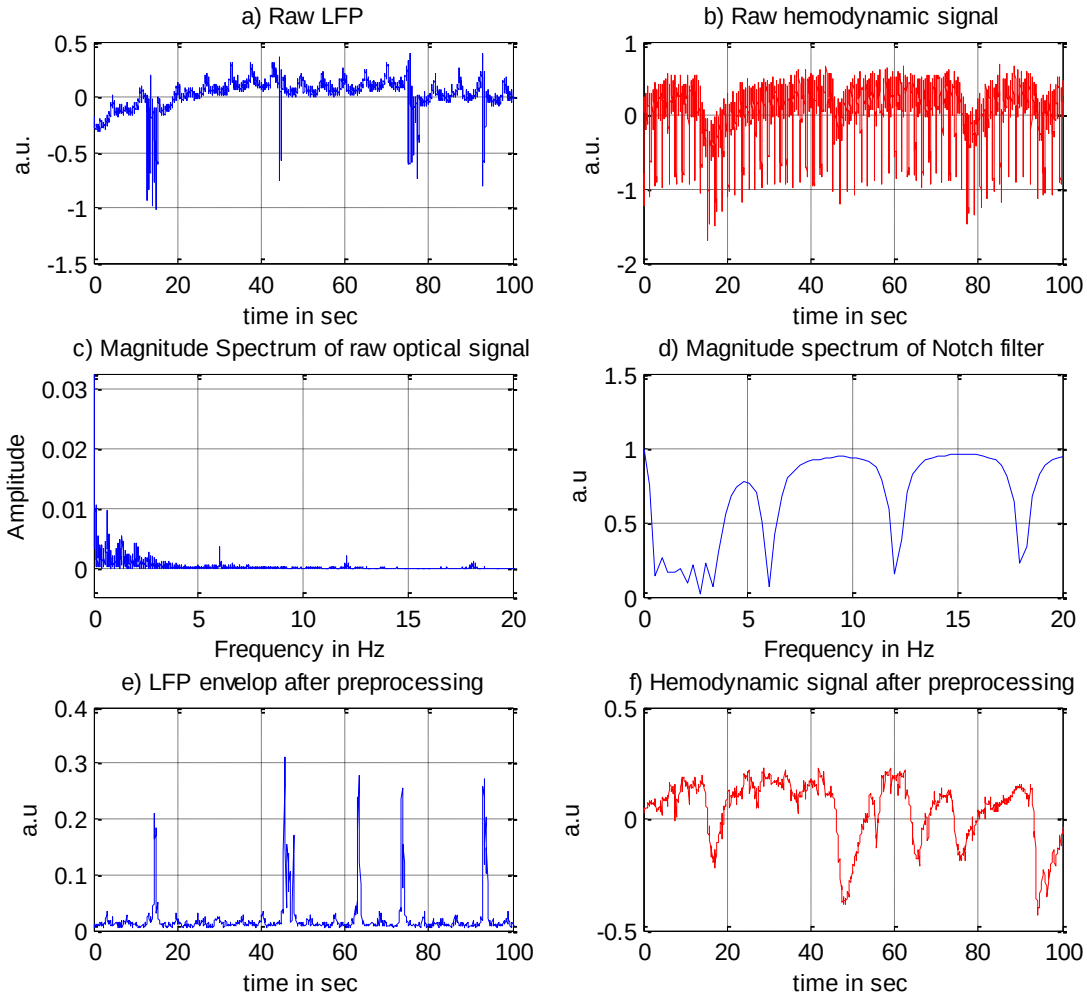

Figure 2-1: Pre-processing pipeline a) Raw LFP envelop b) Raw optical signal c) Power Spectrum of optical signal showing cardiac noise peaks at multiples of 0.6Hz and respiratory noise peak at 6Hz d) Magnitude response of notch filter with notches at appropriate peaks e) LFP envelop after pre-processing d) Optical signal after pre-processing

3. HRF ESTIMATION

At this stage, the problem is to study the system whose input is the LFP envelop and output is optical measured hemodynamic signal.

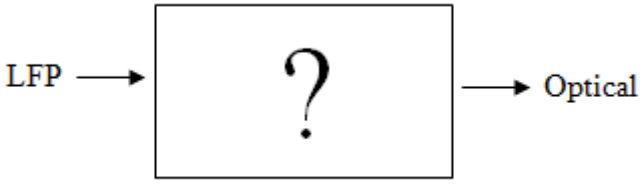

We assume a linear time invariant (LTI) model for the system. The impulse response of the LTI model is called the Hemodynamic Response Function (HRF). In this chapter, we describe the method of estimating the HRF and its optimal order. The estimated HRF with its optimal order will be used to fulfill our study objectives in subsequent chapters.

3.1 METHODS

The method of least-square filtering was used to find an estimate of hemodynamic response function (HRF). Minimum Description Length (MDL) criterion was used to determine the optimal order of the estimated HRF.

3.1.1 Least-square filtering & its relation with MMSE

[14] Let x[n]: LFP envelop, y[n]: optical signal and let h[n]: impulse response of the unknown system so we assume

$$y[n] = x[n] * h[n] + w[n] \quad (1)$$

Where w[n]: white Gaussian noise with zero mean and variance σ^2.

We further assume that x[n] and y[n] are jointly wide sense stationary processes i.e. $r_{xx}(n, n-k) = r_{xx}(k), r_{yy}(n, n-k) = r_{yy}(k)$ and $r_{xy}(n, n-k) = r_{xy}(k)$. We find the minimum mean square estimate (MMSE) of h[n] i.e. let

$$y^{'}[n] = x[n] * h^{'}[n] = \sum_{l=0}^{M2} h^{'}[l]x[n-l] \tag{2}$$

$$e[n] = y[n] - y^{'}[n] \tag{3}$$

$$\min E[e^2[n]]$$

$$\boldsymbol{h}'[\boldsymbol{n}] = R_{xx}^{-1} \times r_{yx} \tag{4}$$

$$R_{xx} = \begin{bmatrix} r_{xx}(0) & r_{xx}(-1) & r_{xx}(-2) & \dots & r_{xx}(-M2) \\ r_{xx}(1) & r_{xx}(0) & r_{xx}(-1) & \ddots & \vdots \\ r_{xx}(2) & r_{xx}(1) & \ddots & \ddots & r_{xx}(-2) \\ \vdots & \ddots & \ddots & r_{xx}(0) & r_{xx}(-1) \\ r_{xx}(M2) & \dots & r_{xx}(2) & r_{xx}(1) & r_{xx}(0) \end{bmatrix} \tag{5}$$

$$\boldsymbol{r_{yx}} = \begin{bmatrix} r_{yx}(0) \\ r_{yx}(1) \\ \vdots \\ r_{yx}(M2) \end{bmatrix} \tag{6}$$

If we further assume that x[n] and y[n] are ergodic processes then the ensemble correlations can be given by time correlations i.e.

$$r_{xx}(k) = \lim_{N\to\infty} \frac{1}{N} \sum_{n=0}^{N} x[n]x[n-k] \tag{7}$$

$$r_{yx}(k) = \lim_{N\to\infty} \frac{1}{N} \sum_{n=0}^{N} y[n]x[n-k] \tag{8}$$

If we have finite amount of data then the time auto and cross correlations evaluated become an asymptotically unbiased estimate of the auto-correlation and cross-correlation functions of the above ergodic processes. In this case least-square filtering in which an estimate of impulse response is found by minimizing the l2-norm of error e[n] is an asymptotically unbiased estimate of the impulse response given by (4). So we find the least-square estimate of the impulse response. From (3)

$$y[n] = y^{'}[n] + e[n]$$

$$y[n] = \sum_{l=0}^{M2} \mathrm{h}^{'}[\mathrm{l}]\mathrm{x}[\mathrm{n} - \mathrm{l}] + \mathrm{e}[\mathrm{n}]$$

$$\begin{bmatrix} y[i1] \\ y[i1+1] \\ y[i1+2] \\ \vdots \\ y[i2] \end{bmatrix} \begin{bmatrix} x[i1] & x[i1-1] & x[i1-2] & \dots & x[i1-M2] \\ x[i1+1] & x[i1] & x[i1-1] & \dots & x[i1-M2+1] \\ x[i1+2] & x[i1+1] & x[i1] & \dots & x[i1-M2+2] \\ \vdots & \vdots & \vdots & \vdots & \vdots \\ x[i2] & x[i2-1] & x[i2-2] & \dots & x[i2-M2] \end{bmatrix} \begin{bmatrix} h'[0] \\ h'[1] \\ h'[2] \\ \vdots \\ h'[M2] \end{bmatrix} + \begin{bmatrix} e[i1] \\ e[i1+1] \\ e[i1+2] \\ \vdots \\ e[i2] \end{bmatrix} \quad (9)$$

$$\boldsymbol{y} = A \times \boldsymbol{h'} + \boldsymbol{e} \quad (10)$$

The indices i1 and i2 are chosen so that all the samples in the A matrix above lie inside the input signal x[n]. For example if M2 = 200, so we choose i1= M2 = 200 so that the most previous sample x [i1-M2] = x [0]. Index i2 is the index of the last sample in the input signal x[n]. This method is called the covariance method in least square filtering [14]. The estimate of impulse response $\boldsymbol{h}^{'}$ is given by $\boldsymbol{h}^{'} = (A^H A)^{-1} A^H \boldsymbol{y}$ for any value of M2. We find the optimal value of M2 using a model order selection technique Minimum Description Length (MDL) [17].

3.1.2 Model order

In order to gain more insight into the problem of model order, we start with an example. Suppose that y is observed which is related to x in the following way

$$y_i = (2 * x_i + 1) + e_i \quad (i = 1, 2, \ldots 9)$$

So the true model or system is represented by a degree 1 polynomial but it is unknown. We fit polynomials of different degrees and use ordinary least squares to find the coefficients of the model. That is the following models are fit

$$y_i^{'} = c_0 + c_1 * x_i$$

$$y_i^{'} = c_0 + c_1 * x_i + c_2 x_i^2 + c_3 x_i^3$$

$$y_i^{'} = c_0 + c_1 * x_i + c_2 x_i^2 + c_3 x_i^3 + c_4\, x_i^4 + c_5\, x_i^5$$

$$y_i^{'} = c_0 + c_1 * x_i + c_2 x_i^2 + c_3 x_i^3 + c_4\, x_i^4 + c_5\, x_i^5 + c_7 x_i^7$$

$$y_i^{'} = c_0 + c_1 * x_i + c_2 x_i^2 + c_3 x_i^3 + c_4\, x_i^4 + c_5\, x_i^5 + c_7 x_i^7 + c_8 x_i^8$$

The actual observations (Figure 3.1a) and the values of $y_i^{'}$ for the same $x_i's$ given by the least square estimate of each of the above models are shown in(Figure 3.1a). If we base our model selection on the "goodness of fit" then the 8th degree polynomial which passes through all the data points exactly is what we should select. However, the true model is a degree 1 polynomial. So we see here that although the 8th degree polynomial fits the data perfectly, it does not represent the true system. In other words if I had another set of observation of $y_i's$ for different $x_i's$ based on the above model and 1st degree and 8th degree polynomials (estimated above) were used to predict the values of $y_i^{'}s$ then the prediction error will be larger for the higher

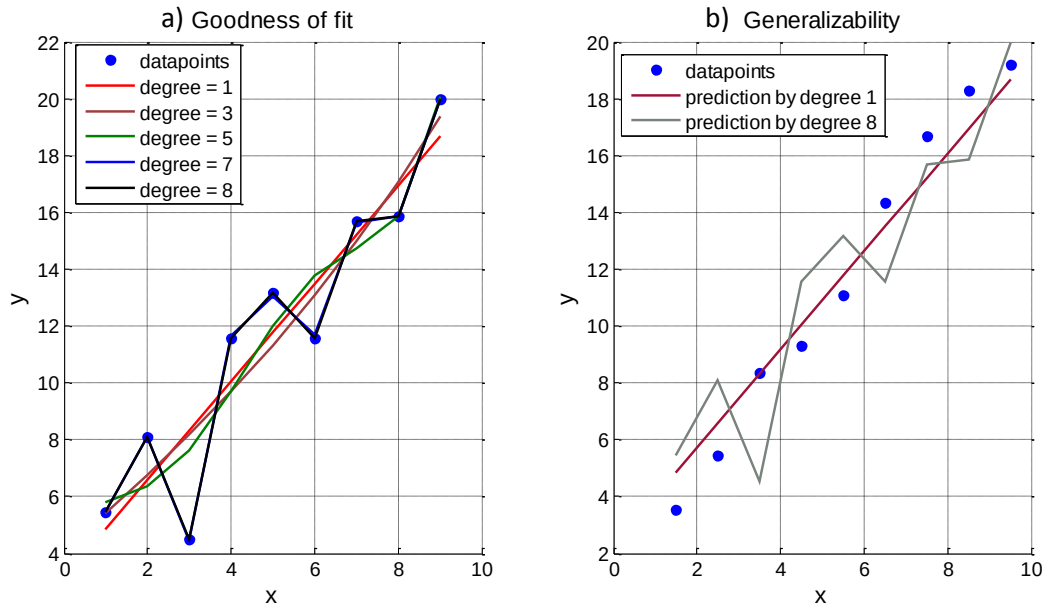

Figure 3-1: a) The actual data points and the polynomial of different degrees estimated by least squares. b) The 1st degree polynomial is more general that the 8th degree polynomial in the sense that the prediction error is smaller

degree polynomial as clear from Figure 3.1b. So although the 8th degree polynomial fits the data perfectly it is not 'general' in the sense that it performs poorly in case of prediction and therefore does not represent the true model. On the other hand 1st degree polynomial does not fit the data perfectly but is more general (Figure 3.1).

The same problem occurs in finding the true model order for the causal impulse response. Referring to eq. (9) as we move towards higher values of M2, more columns are added in the above matrix which is equivalent to finding an estimate of $y[n]$ in a larger vector space which is bound to reduce the residual sum of squares (RSS) or variance of the error e[n] (σ_e^2). When the number of independent columns equal i2-i1 then the error will be zero. However, after the true value of M2, say M2*, the reduction in σ_e^2 caused as a result of including another parameter would be extremely small because as much as could be explained of the output y[n] by the

convolution part of the model i.e. $\sum_{l=0}^{M2} h'[l]x[n-l]$ would have been explained and what would be left is noise. In other words, the additional parameter would not explain any systematic variation. So if there were a criterion that compares the reduction in σ_e^2 for every additional parameter included against the total number of parameters, an insignificant reduction in variance would make the inclusion of this new parameter unjustified. One such criteria is the Minimum Description Length (MDL) given by (for least square criterion)

$$MDL(P) = N * log(\sigma_P^2) + P * logN$$

$P: model\ order, \sigma_P^2 : variance\ of\ error\ for\ order\ P, N: number\ of\ observations$

We use an example to explain the working of this criterion. Suppose that h[n] is a known causal filter of order 180, x[n] is simulated local field potential envelop and y[n] is the convolution of h[n] and x[n] plus some white gaussian noise. We define a window from [10, 300] and for each integer in this window find the least square estimate of h[n] for that value of order and compute MDL for each order as well. Figure 3.2 shows plots of individual terms and the overall MDL. As expected initially when the order is increased there is a large decrease in error variance indicated by the large negative slop of the red curve. At this point the negative slope of the first term dominates and MDL also decreases. However, once we are around the true model order the decrease in variance is just too small and the second term begins to dominate causing MDL to increase. This way the true model order is the one at which MDL is minimum which for the example case considered turns out to be 176 which is quite close to 180.

The optimal model order for HRF can be found using the same procedure. The BOLD response to a short-duration stimulus in task based studies has been reported to last for around 18-20 seconds [16] corresponding to a length of 180-200 samples for a sampling rate of 10Hz. We

define a window to search within for the optimal model so that the length of 200 samples is included in it. We used window of 10-800 samples. For each value of M2 in this window, the HRF is computed using least-square filtering eq. (9) and (10) and the value of MDL is computed for that M2. The order which gives the minimum value of M2 is the optimal order.

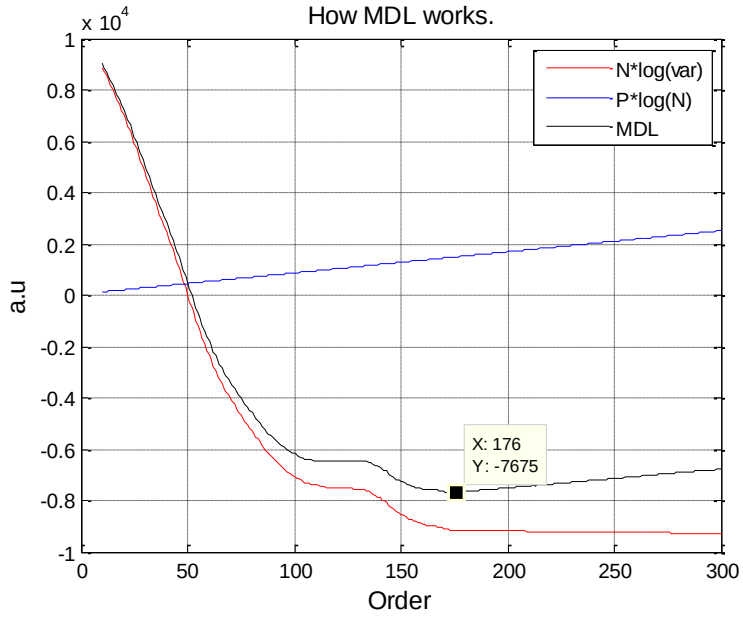

Figure 3-2: The red curve indicates the first term of MDL. Its decrease is large when far from the correct model but close to it becomes almost flat. The blue line indicates the second term of MDL which begins to dominate when close to the true model. The black curve is the overall MDL

3.2 RESULTS & DISCUSSION

Figure 3.3 shows the plots of MDL vs. model order for different subjects. The window in which the model order was searched is [10, 800]. Two curves for a subject represent the different runs of the same subject. Although the model order across runs is not exactly the same but for both runs of all subjects the model order is between 100 and 200. From this it can be concluded that when modeling the system between LFP envelop which corresponds to synaptic activity and hemodynamic response by an LTI system represented by a causal impulse response, the optimal

order is somewhere between 100 and 200. The maximum optimal model order is obtained for run # 02 of subject 03 which is approximately 200 (Figure 3.3c). Therefore we estimate the HRF for M2*= 200 and use this HRF in subsequent chapters for investigating linearity and causality. Choosing the maximum from among optimal orders for different subjects ensures that we do not under fit in any case. Figure 3.4 shows a HRF estimated for model order of 200.

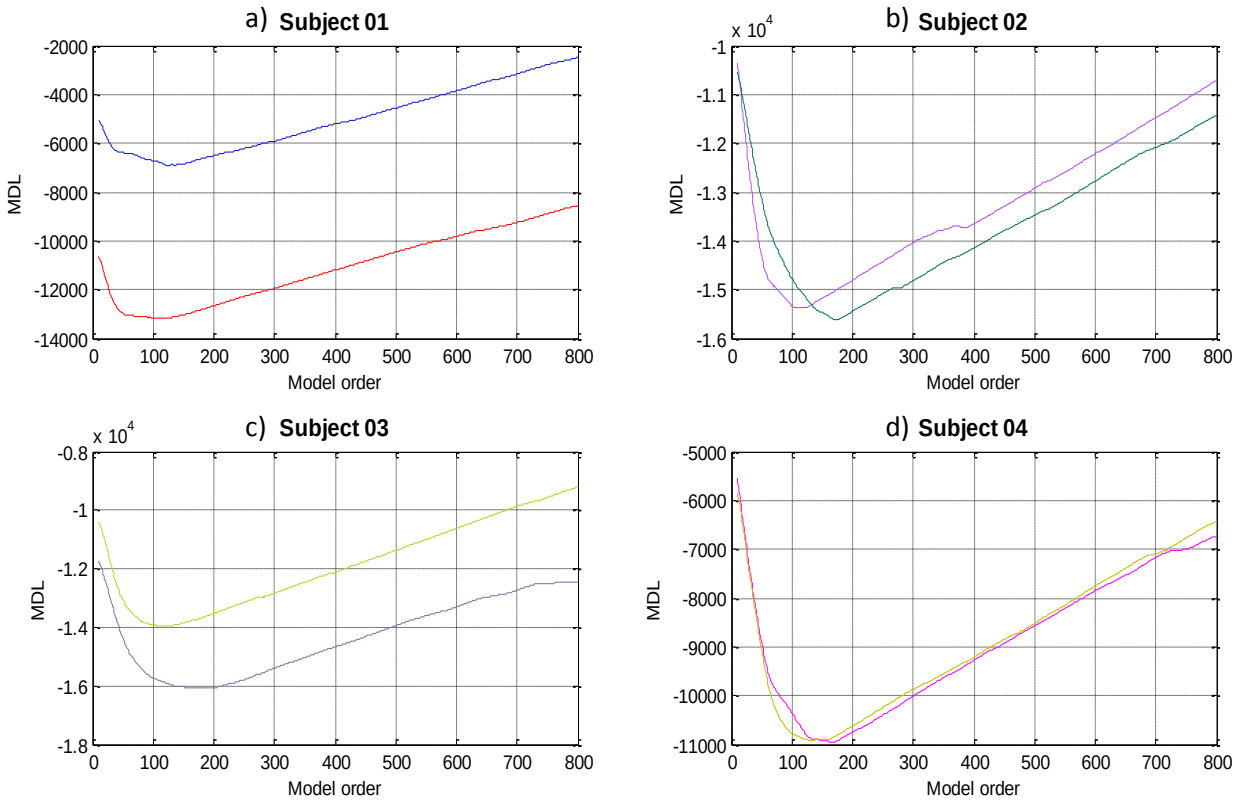

Figure 3-3: MDL for two runs of different subjects. a) Subject 01 b) Subject 02 c) Subject 03 d) Subject 04 The different colors in each plot indicate the correspond to different runs

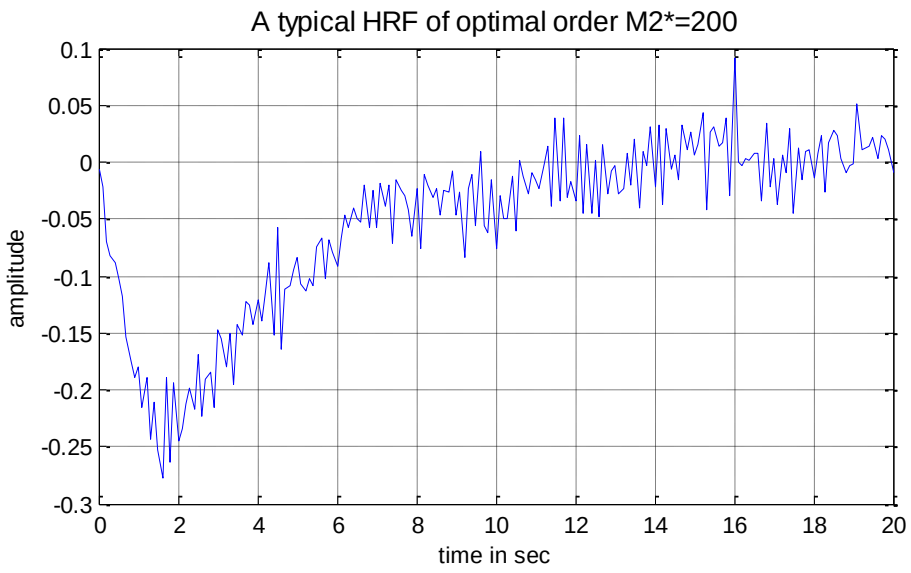

Figure 3-4: HRF of optimal order

3.3 CONCLUSION

The estimated HRF as expected indicates that there will be a decrease in the optically measured hemodynamic response in response to a short duration neural activity burst. This corresponds to the dip in the optically measured hemodynamic response signal (Figure 3.1b). Secondly, the estimated HRF peaks at around 2 sec (Figure 3.4) which is in agreement with HRF peak time reported by previous studies [16]. The optimal order is somewhere between 100 to 200 with the maximum optimal order equal to 200.

4. INVESTIGATING LINEARITY OF HRF DURING RESTING STATE

[1] showed that the relationship between BOLD response from human visual cortex due to stimulus and neural activity is non-linear for small inter-stimulus interval (ISI). They observed the BOLD response to paired-stimuli having small to large ISIs. A subtracted response was obtained by subtracting from the paired-response (corresponding to each ISI) the response due to single stimulus. If the underlying system were linear, the subtracted response should have been the same as the BOLD response to a single stimulus. But it was shown that the peak value attained by the subtracted response was much smaller than that of single stimulus response for small ISIs. [3] showed that the estimated impulse response of an LTI model changed with stimulus duration and that the response obtained by superposition of responses of smaller, shifted stimuli does not match the response to a longer stimulus. Motivated by these methods, we have adapted two approaches to investigate linearity in resting state.

4.1 METHODS

We utilize two methods for investigating linearity of HRF under resting state condition.

4.1.1 Approach no. 1

The first approach makes use of the superposition principle. According to the superposition principle, if the response of an LTI system to input $x_1[n]$ is $y_1[n]$ and that due to $x_2[n]$ is $y_2[n]$ then the response to $\alpha\ x_1[n] + \beta\ x_2[n]$ is $\alpha\ y_1[n] + \beta\ y_2[n]$. We identify the portion of LFP envelop such that we have a group of close by neural activity bursts. A group is defined as neural activity bursts less than 12s apart from one another. The optically obtained hemodynamic response corresponding to this group of bursts is also extracted. We then find a ‘predicted

response' which corresponds to the superposition of responses to individual bursts in the group. The predicted response is obtained by convolving the group of LFP envelop with HRF estimated using isolated bursts and their optical responses by the method of least square using M2*=200. A burst is defined as isolated if there is no other neural activity burst 15s before or after it. The hypothesis is that if the underlying system is non-linear and if there is a kind of saturation in BOLD response as reported for task-based studies [1] then the predicted response must overestimate the actual response consistently. The inter burst intervals (IBIs) are as small as 1or 2s which are the same as used in previous studies. If such overestimation is not observed on a consistent basis, it can be concluded that during resting state the relationship between neural activity and BOLD signal is linear.

4.1.2 Approach no. 2

In previous research [3] it was shown that the estimated HRF changed with an input parameter (stimulus duration). Following this we investigate whether in case of resting state the estimated impulse response changes as average width of neural activity bursts changes taken over a window. The hypothesis is that if the estimated HRF changes with average burst width it will indicate, like in [3] that the underlying system is non-linear. Whereas if it does not change, it would corroborate that the unknown system is time invariant.

We used the method of sliding window recursive least square (sliding RLS). We find a least square estimate of the impulse response over time using the input LFP envelop and output optical signal falling in a window. The size of the window is chosen so that it includes at least one LFP burst and the corresponding output. This window is then slided ahead by enough samples so that the autocorrelation of the output optical signal has become small. Then another

least-square estimate of impulse response is found using data falling in the window at this new location. The idea is illustrated in Figure 4-1 below.

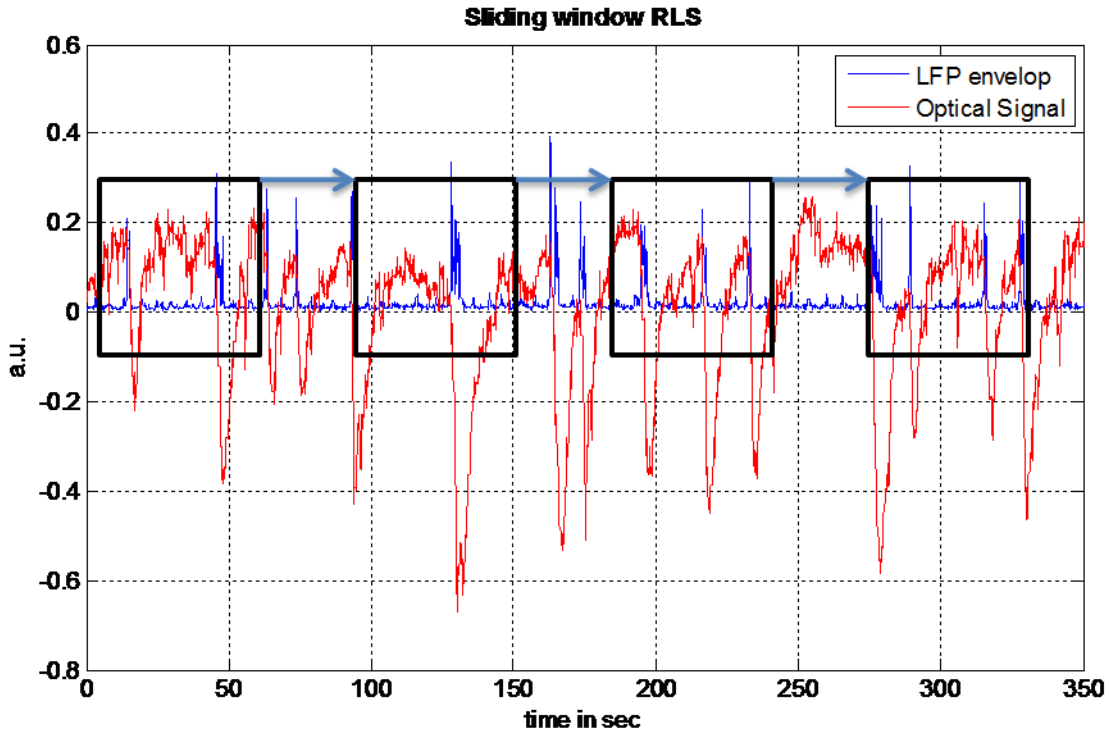

Figure 4-1: Sliding window RLS. The red curve shows the optical signal and the blue curve the LFP envelop. Optical signal and LFP envelop falling in the black windows are used to estimate the impulse response. The average burst width is also calculated for each window.

In order to compare the different impulse responses from one another we use the following parameters: full-width half maximum (FWHM), time-to peak (Tpk) and peak value (Pk) ([2]). Then we find their correlation coefficient with the average burst width calculated for each window. The window length is chosen so that at least one LFP envelop lies in it and the window separation is chosen so that the output auto-covariance is as small as possible. The parameters are not entirely uncorrelated since the window separation is limited by the number of data points. Moreover, t-test is performed to evaluate whether the observed correlation are statistically significant i.e. whether we will observe a correlation say different from zero consistently if we

repeat the above procedure a large number of time for different data sets. In t-test, we assume a null hypothesis H_0 and an alternate hypothesis H_a. In our case

H_0: *the correlation between average burst width and impulse response parameters is zero*

H_a: *the correlation between average burst width and impulse response parametrs is different from zero*

Assuming the null hypothesis is true the correlation ρ is supposed to follow a t-distribution and the probability of getting a correlation value greater than or equal to the observed value is found. This probability is called the p-value. If the p-value is greater than a threshold which is called the significance level (α usually 0.05 or 0.025) then we fail to reject the null hypothesis which implies that the observed correlation are not statistically significant. Although the t-test requires that the impulse response parameters for adjacent windows and average burst width measurements for adjacent windows are independent or at least their auto-covariance is zero which is not the case here. However, in case the adjacent impulse response parameters and adjacent average burst-width have non-zero auto-covariance, the probability of getting a high cross-correlation between impulse response parameters and burst-width under null hypothesis is higher. In other words the null distribution is broader and hence the effective p-value is even larger then what we observe. Hence we can make correct inferences from t-test even in our case.

The change in HRF with another parameter of the input LFP envelop i.e. burst crowdedness was also investigated. Two least square estimates, one corresponding to that portion of LFP where the neural activity bursts were extremely crowded and the other corresponding to that portion of the LFP envelop where the bursts were sparse were found. The 95%-confidence interval for each estimate was also computed. The 95% confidence interval has 0.95 probability of containing the

true impulse response. If the true impulse responses for the two different cases are same then the corresponding confidence intervals should have large overlap. Whereas a large difference between the two confidence intervals would indicate that the impulse response estimate depends on the crowdedness of burst and hence the unknown system is time-variant.

4.2 RESULTS & DISCUSSION

Figure 4.2 shows the actual and predicted responses for different subjects and the associated group of LFP envelop. The first important observation is that the actual and predicted responses match well. Secondly, there is no clear evidence of non-linearity as indicated for task based case in previous studies [1]. The red circle highlights places where the predicted response over-estimates the actual response and the green circle highlights places where it underestimates. As can be seen, there is no consistent behavior of either over-estimation or under-estimation across subjects. From these observations we conclude that LTI model works well for our unknown system and that there is no clear evidence of non-linearity in resting-state opposed to what has been reported for task based studies [1].

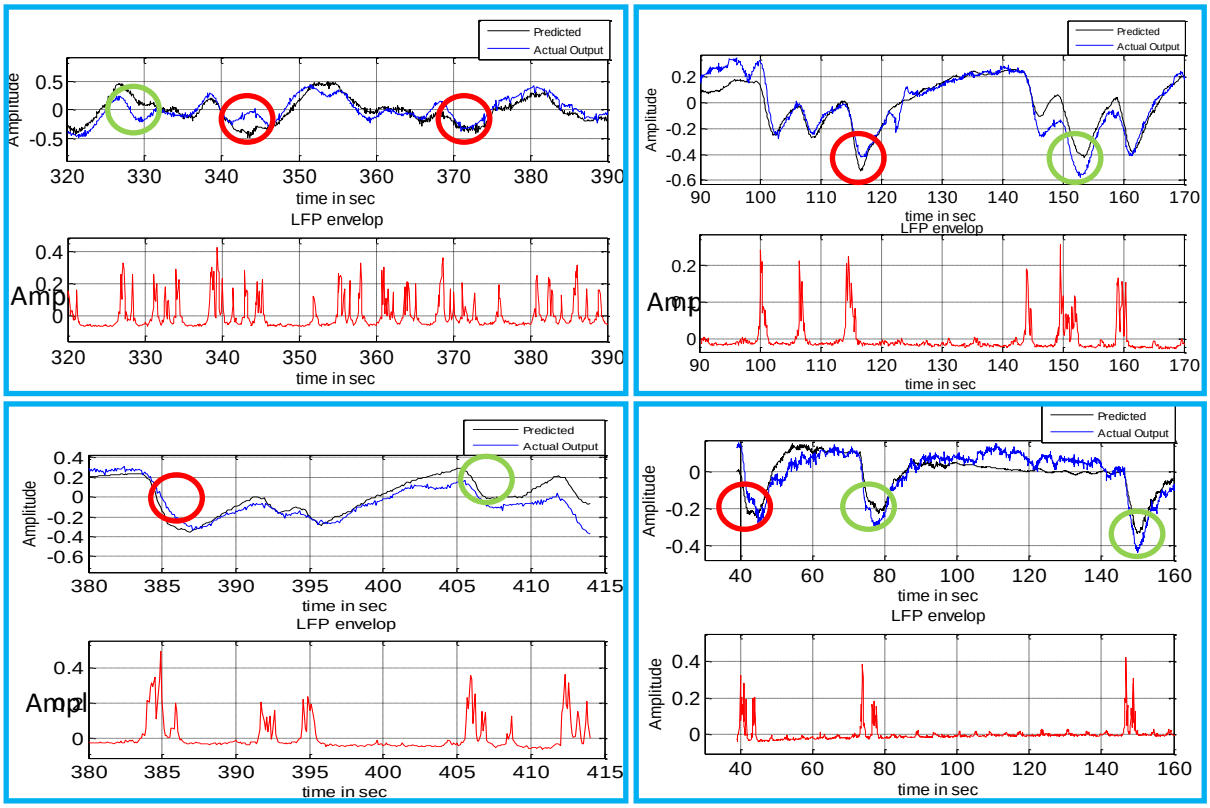

Figure 4-2: Each panel has two plots. The top plot in each panel shows the predicted output in black and the actual output in blue. The bottom plot shows the corresponding local field potential (LFP) envelops with which the estimated hemodynamic response was convolved to get the predicted response

Table 4-1shows correlation coefficient and their corresponding p-values obtained via t-test for parameters FWHM, Tpk and Pk for each of the six subjects. Under 2.5% significance level, it can be observed that all the p-values for each subject are greater than 0.025 and the effective p-value is also greater. This shows that the least-square estimates obtained over time do not depend on the mean burst width and that the unknown system is time-invariant.

Table 4-1: Correlation between average burst width and HRF parameters and their corresponding p-values

	FWHM		Time to peak		Peak Value	
Subject	Correlation	p-value	Correlation	p-value	Correlation	p-value
1	0.4715	0.238	-0.7055	0.0506	0.5247	0.1819
2	-0.7325	0.2675	-0.7247	0.2753	0.5415	0.4585
3	-0.1089	0.8373	-0.5028	0.3094	0.1469	0.7812
4	-0.4864	0.1292	0.1429	0.675	0.4833	0.1321
5	0.4399	0.1757	0.0263	0.9389	0.0245	0.9431
6	0.4956	0.1452	0.5133	0.1291	0.0416	0.9092

Figure 4-3: shows two impulse response estimates in green and black corresponding to green and black colored windows. These estimates correspond to average inter-burst interval LFP envelop. The brown color in the figure 4.3b shows the overlap between the 95% confidence intervals of the two estimates. The overlap is large which again shows that the impulse response estimate of the unknown system does not depend on the IBI and hence LTI model is a good fit for it.

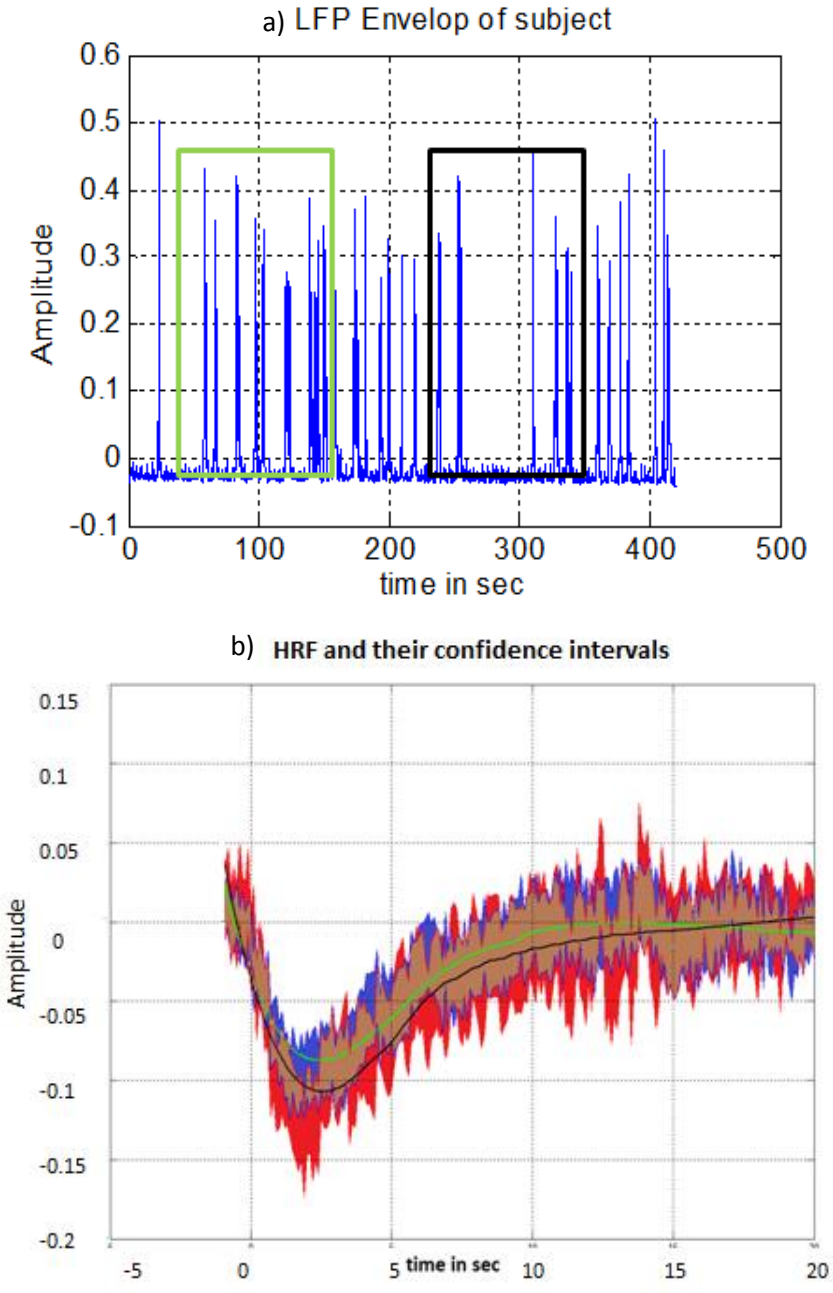

Figure 4-3: a) Local field potential envelop of a subject with two windows. The green window corresponds to high mean inter-spike interval and the black window corresponds to low mean inter-spike interval. b) The corresponding smoothed HRFs are show in green and black respectively in the plot on bottom-left. This plot also shows in blue and red colors confidence intervals of the two HRFs. The brown color represents the area of intersection of the two confidence intervals.

4.3 CONCLUSIONS

The relationship between LFP envelop and optically measure hemodynamic response does not show any non-linearity during resting-state. The actual output and the predicted output obtained by convolving the estimated HRF with group of bursts matched well. No consistent over or underestimation was observed. Moreover, HRF does not vary with change in the average burst width or the burst crowdedness. It can be concluded that in case of resting state LTI system serves as a good model between neural activity and hemodynamic response.

5. INVESTIGATING CAUSALITY OF HRF DURING RESTING STATE

Neural activity and the change in concentration of oxygenation (hemodynamic signal) during resting state are spontaneous. There is no overt task or stimulus to drive them. However, there is a spontaneous fluctuation in the tone of blood vessels in the brain which is independent of heartbeat, respiration and innervations called vasomotion [18]. It is possible that a third common mechanism derives this spontaneous fluctuation and drives both the neural activity and oxygenation change during resting state. Or that vasomotion derives the neural activity and hemodynamic signal during resting state. This opens up the possibility that the BOLD response in a brain region during resting state may begin before the onset of neural activity since a third common mechanism is controlling both of them. In other words it is possible for the HRF during resting state to be non-causal contrary to task-based paradigm. We investigate this possibility in this chapter. Moreover it is possible that hemodynamic signal may also have some causal influence on the neural activity. Causal influences from LFP to BOLD have been previously studied [12]. However, our work differs in the sense that we also consider the presence of noise inherent in signals (LFP, BOLD) and look into how they may affect conclusions regarding causality in context of fMRI studies.

5.1 METHODS

5.1.1 Least-square filtering

In order to investigate whether HRF can be non-causal, optical obtained hemodynamic signal y[n] is modeled as the convolution of LFP envelop x[n] with a non-causal impulse response plus some gaussian zero mean white noise

$$y[n] = \sum_{l=-M1}^{M2} h^{'}[l]x[n-l] + e[n] \tag{11}$$

The impulse response ***h[l]*** = $[h(-M1) \quad h(-M1+1) \quad \ldots \quad h(0) \quad \ldots \quad h(M2-1) \quad h(M2)]$ is non-causal from M1 to M2. M2 = M2*=200 and M1 = 10 corresponding to 1s duration for the above sampling frequency. The choice of M1 is arbitrary since we are interested in investigating whether the hemodynamic response can be non-causal or not. The least square criterion is used to find the filter estimate. As discussed in the chapter on linearity, the least-square is asymptotically unbiased estimate of the weiner filter in case the random processes y[n] and x[n] are assumed wide-sense stationary and ergodic. The formulation for the least square is shown below.

$$\begin{bmatrix} y[i1] \\ y[i1+1] \\ y[i1+2] \\ \vdots \\ y[i2] \end{bmatrix} =$$

$$\begin{bmatrix} x[i1+M1] & x[i1-1+M1] & x[i1-2+M1] & \ldots & x[i1-M2] \\ x[i1++M1+1] & x[i1+M1] & x[i1-1+M1] & \ldots & x[i1-M2+1] \\ x[i1+M1+2] & x[i1+1+M1] & x[i1+M1] & \ldots & x[i1-M2+2] \\ \vdots & \vdots & \vdots & \vdots & \vdots \\ x[i2+M1] & x[i2-1+M1] & x[i2-2+M1] & \ldots & x[i2-M2] \end{bmatrix} \begin{bmatrix} h^{'}[-M1] \\ h^{'}[1-M1] \\ h^{'}[2-M1] \\ \vdots \\ h^{'}[M2] \end{bmatrix} +$$

$$\begin{bmatrix} e[i1] \\ e[i1+1] \\ e[i1+2] \\ \vdots \\ e[i2] \end{bmatrix}$$

$$\boldsymbol{y} = A \times \boldsymbol{h}' + \boldsymbol{e}$$

$$\boldsymbol{h}^{'} = (A^H A)^{-1} A^H \boldsymbol{y}$$

i1 and i2 are chosen according to the covariance method [14]described in previous chapter so that all the data points i.e. the x[k] in the matrix A are taken from the given data and are not assumed zero.

5.1.2 Validating the least-square filtering approach

The least square approach for investigating causality of hemodynamic response function (HRF) described above assumes that the input LFP envelop x[n] is noise free. In this section we investigate the effect of noise in input on causality of HRF.

(1) Theory

Let's try to see mathematically the effect due to presence of noise in input. Let

$f[n]: true\ input$

$x[n]: noisy\ input = f[n] + w_1[n]$ (Where $w_1[n]$ is zero mean i.i.d gaussian noise)

$y[n] = h[n] * f[n] + w_2[n]$ ($w_2[n]$ is zero mean i.i.d gaussian noise)

The least square estimate found using y[n] and x[n] is an asymptotically unbiased estimate of Weiner filter if we assume that the processes y[n] and x[n] are wide sense stationary and ergodic. Therefore to analyze the effect of noise we find the minimum mean square estimate (MMSE) of h[n]. That is we find h'[n] such that

$$y'[n] = h'[n] * x[n] = \sum_{k=-\infty}^{\infty} h'[k]x[n-k]$$

$$e[n] = y[n] - y'[n]$$

$$\min E(e^2[n])$$

From [13]

$$H'(jw) = \frac{P_{yx}(jw)}{P_{xx}(jw)} \ or\ H'(z) = \frac{P_{yx}(z)}{P_{xx}(z)}$$

$$r_{yx}[k] = E(Y[n]X[n-k]) = E\big((h[n] * f[n] + w_2[n])(f[n-k] + w_1[n-k])\big)$$

$$= h[n] * r_{ff}[n]$$

$$\therefore P_{yx}(z) = H(z)P_{ff}(z)$$

$$r_{xx}[k] = E\big((f[n] + w_1[n])(f[n-k] + w_1[n-k])\big) = r_{ff}[k] + \sigma_{w_1}^2$$

$$\therefore P_{xx}(z) = P_{ff}(z) + \sigma_{w_1}^2$$

$$\therefore H'(z) = H(z)\frac{P_{ff}(z)}{P_{ff}(z) + \sigma_{w_1}^2} = H(z)H_d(z) \tag{12}$$

As can be seen from (12) the estimated Weiner filter will be different from the true impulse response. In fact the estimated impulse response will be a blurred version of the actual impulse response since it gets convolved with $h_d[n]$.

(2) Simulation

Simulations were also used to investigate the effect of noise on causality of HRF. The idea is to obtain an output y[n] by convolving a noise free input f[n] with a known causal HRF h[n] and add some white noise to the result of convolution. Then use x[n] which is f[n] plus some white noise and y[n] to estimate the HRF h'[n] using the non-causal formulation of least-square filtering in which we take M2 as the order or the true HRF and M1=10 samples. We expect the coefficients of h'[n] before t=0 sec to be zero since h[n] is causal. On the other hand, non-zero coefficients would indicate that noise makes least-square estimate biased.

We need two LFP envelops one noise free and the other noisy. We take the noise free envelop to be a square wave (figure 5.2a).

The noisy LFP envelop is obtained in the following manner. White noise is band-pass filtered between 1-30Hz and the result is multiplied by the square wave envelop to get a simulated LFP signal (Figure 5.2b). The envelop of the simulated LFP down-sampled to 10Hz serves as the noisy envelop (Figure 5.2c). Then a simulated hemodynamic signal is obtained by convolving the true envelop (also down-sampled to 10Hz) with a known causal impulse response (figure 5.2d) and adding some white noise. Finally, the noisy down-sampled envelop and this simulated hemodynamic signal are used to find a least-square estimate of the true impulse response. This simulation is run 100 times and 100 least-square estimates of the true causal impulse response are obtained. T-test is performed to check the statistical significance of the impulse response before t= 0s. The whole process is illustrated in the figure 5.2.

5.2 RESULTS AND DISCUSSION

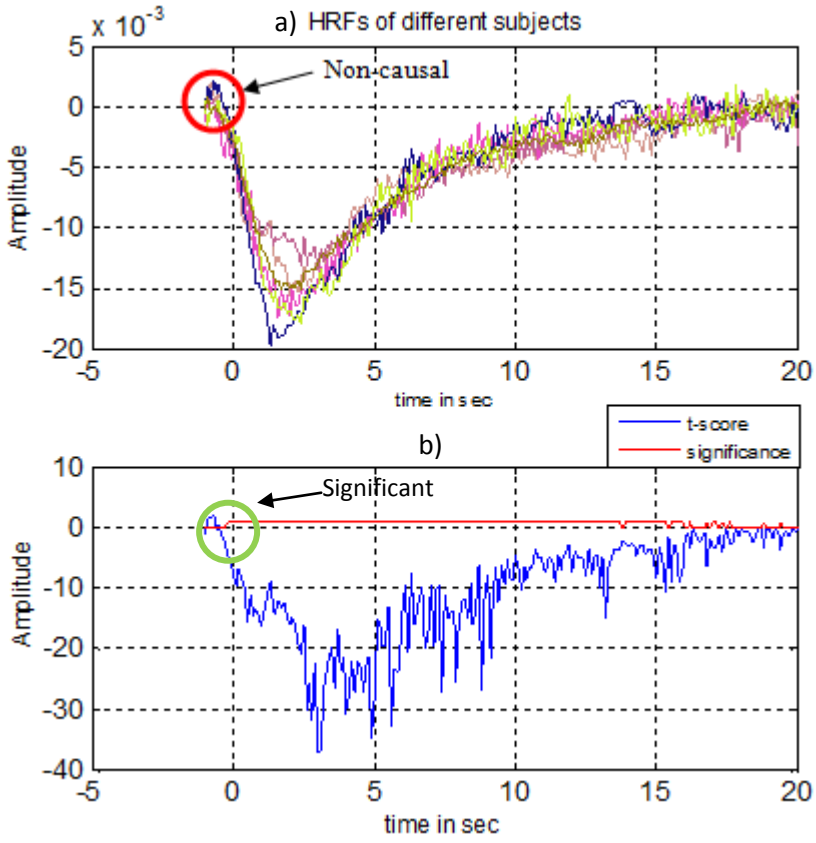

Figure 5-1: HRFs of different subjects. a) All the HRFs are non-zero for t<0 sec. b) The significance level for HRF coefficients. As can be seen even for t<0s, the t-scores are large and they are significant as indicated by the non-zero value of the red curve.

Figure 5-1 shows the HRFs of different subjects estimated using the non-causal implementation of least-square filtering. As shown in 5.1a all HRFs had non-zero coefficients before t=0sec. Moreover, t-test was performed to test the null hypothesis H_0 that the impulse responses are not non-causal versus the alternate hypothesis H_a that they are with a significance level of 5%. As shown in figure 5.1b, the t-test rejects the null-hypothesis for some portion before t=0s as well.

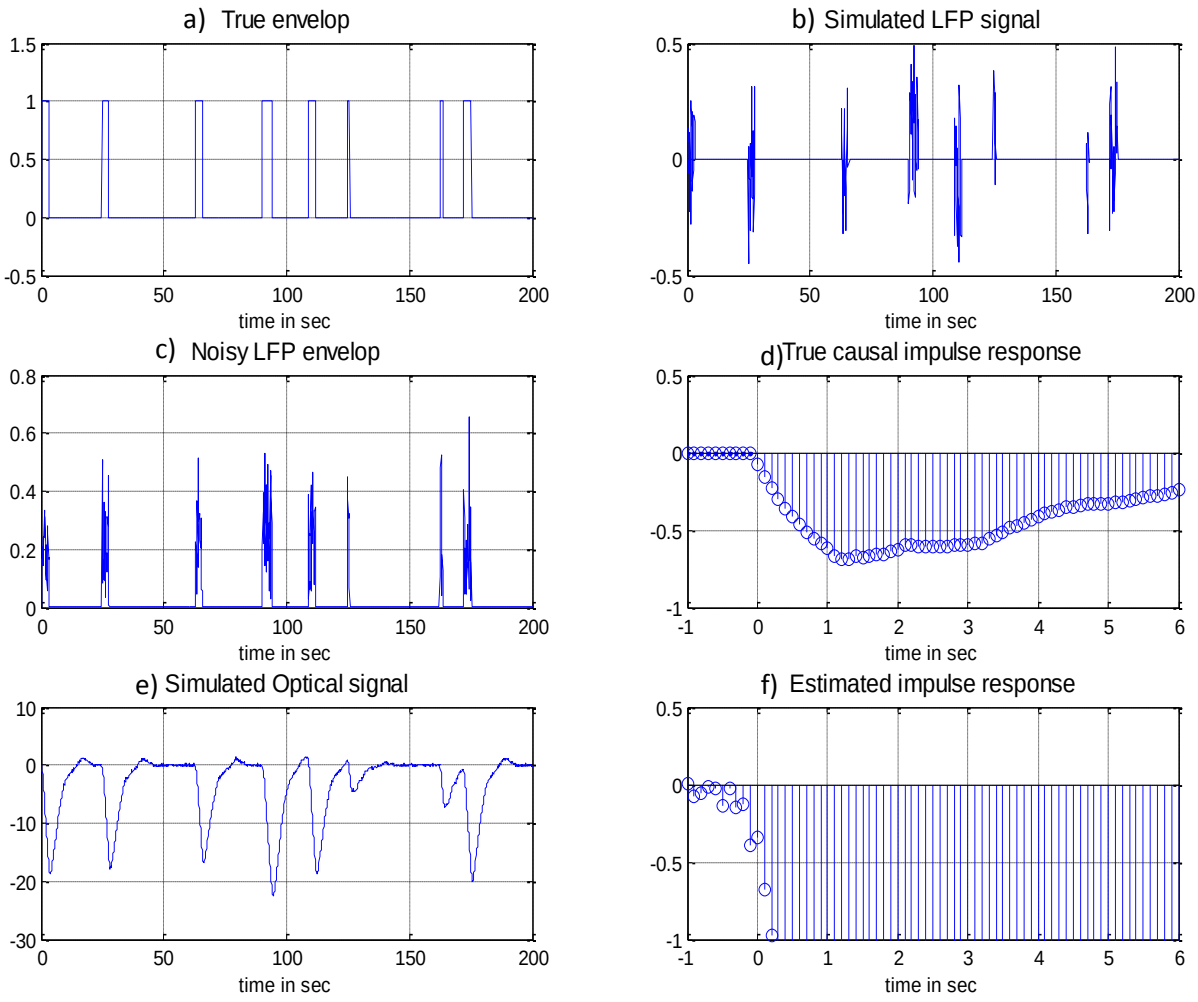

Figure 5-2: An illustrative description of the simulation used to check the effect of noisy envelop on the non-causality of estimated impulse response. a) Noise free square wave envelop b) simulated LFP c) Noisy LFP envelop d) True known impulse response e) Simulated optical signal f) Estimated impulse response turns out to be non-causal

However, eq. (12) tells us that even when y[n] represents the output of a linear time invariant system, the Weiner filter is not equal to the true impulse response. It is the product of H(z) and $H_d(z)$. If $\sigma_{w_1}^2 = 0$ then $H'(z) = H(z)$. $H_d(z)$ performs the function of removing noise from x[n] to find an estimate of f[n] since it has a high response for the frequencies where the power spectral density of f[n] is high. Then this estimate of f[n] is convolved with h[n] to find y'[n] that gives the minimum mean square error. This two step procedure also makes intuitive sense. Since y[n] is originally the convolution of h[n] with f[n], an MMSE estimate should also try to

represent y'[n] as the convolution of h[n] with f[n]. But since x[n] is a noisy version of f[n], the weiner filter first removes noise from x[n] and then convolves the result with h[n]. $H_d(z)$ is also a zero-phase filter and therefore represents a two-sided even sequence in time domain. This can be seen because for an even signal s[n] =s [-n] in time domain the Z-transform satisfies the property that S(z) = S(1/z). Here

$$H_d\left(\frac{1}{z}\right) = \frac{P_{ff}\left(\frac{1}{z}\right)}{P_{ff}\left(\frac{1}{z}\right) + \sigma_{w_1}^2} = \frac{P_{ff}(z)}{P_{ff}(z) + \sigma_{w_1}^2} = H_d(z)$$

$$P_{ff}(z) = P_{ff}\left(\frac{1}{z}\right) \; since \; r_{ff}[k] is \; an \; even \; sequence$$

Therefore in time domain h'[n] is the convolution of the true impulse response with a two-sided sequence. So even if the original impulse response is causal, the presence of noise will cause the estimate to be non-causal. This can also be seen in the results of simulation in figure 5.2f where the estimated impulse response is non-causal whereas the true impulse response is causal.

5.3 CONCLUSION

The above result can mean two things. Firstly, it could mean that the statistically significant non-causality of the impulse response of the LTI model is artifactual and in fact the impulse response is causal. But it is also very possible that the impulse response is in fact non-causal and the presence of noise only enhances this effect. To say anything for sure it is needed that the effect of noise is isolated as a bias adding to the original impulse response of the system. Using [5] as reference, a simulation was created to estimate the bias due to presence of noise in the least square estimate of a system for a known causal impulse response. The bias was estimated and subtracted from the least-square estimate to obtain a bias-compensated least square filter. The

results are shown in Figure 5.3. As can be seen the bias is largest for t<0s and for t>0s it oscillates about zero (5.3d). Moreover, bias-compensated least square estimate is still non-causal (5.3c). Although the coefficients are smaller as compared to that of least-square estimate for t<0s but they are still non-zero and also statistically significant (Figure 5.4). Based on the referenced paper it is only possible to estimate the bias. Finding the true bias requires an infinite number of observations even when the true impulse response is known. Although a large number of observations (10,000) were simulated, it is still not possible to conclude whether or not the true system is non-causal or not. However, a large bias before t=0 sec makes clear the need for practicing caution while making inferences about physiological systems in studies related to causality.

Secondly, eq. (12) shows that popularly used techniques such as least square filtering and weiner filtering will give bias estimates of impulse responses in presence of noise. What this means is that the inferences about underlying physiological systems made in studies related to neuroscience and fMRI based on impulse response estimates (e.g. the hemodynamic response function) may not be entirely accurate and the effect of noise in signals of interest has to be kept in mind.

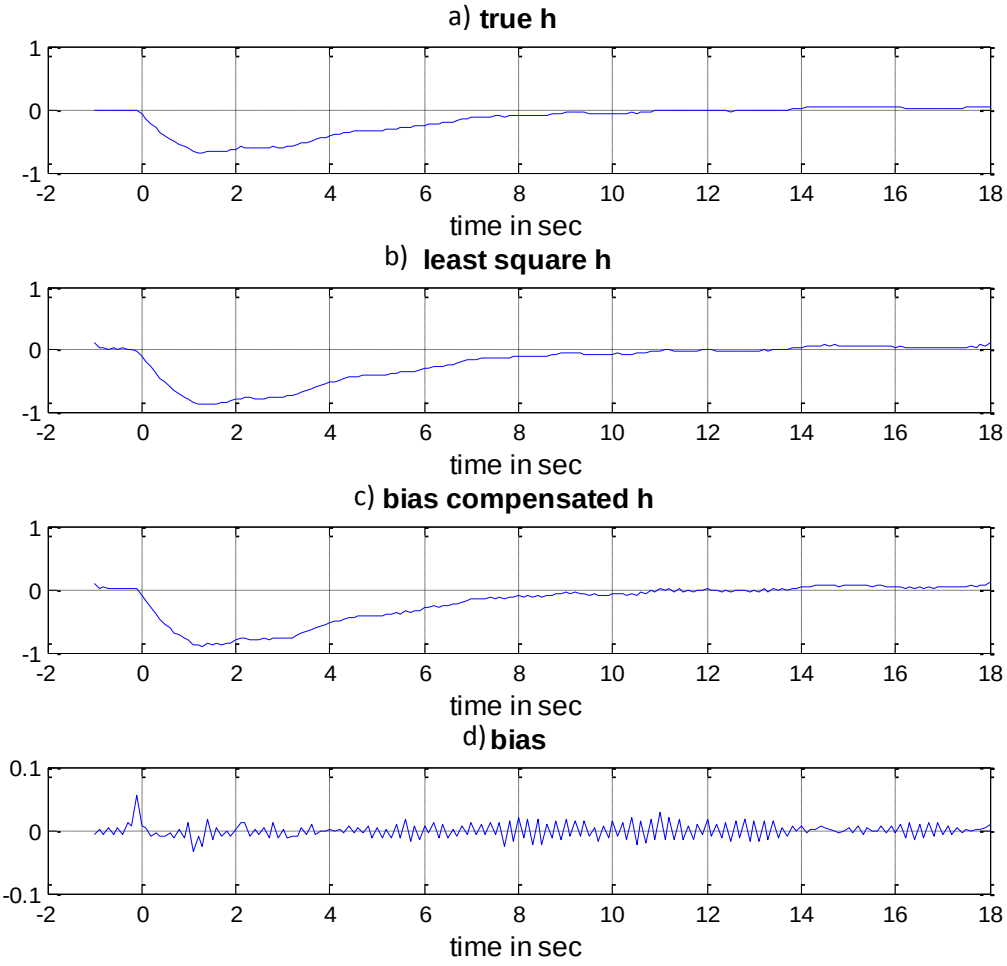

Figure 5-3: a) shows the true simulated impulse response which is zero for t<0. b) shows the least-square estimate. The last panel shows the estimate of bias that is present in the least-square estimate. c) shows the bias-compensated least square estimate obtained by subtracting the bias estimate from the least-square estimate d) bias in LS estimate

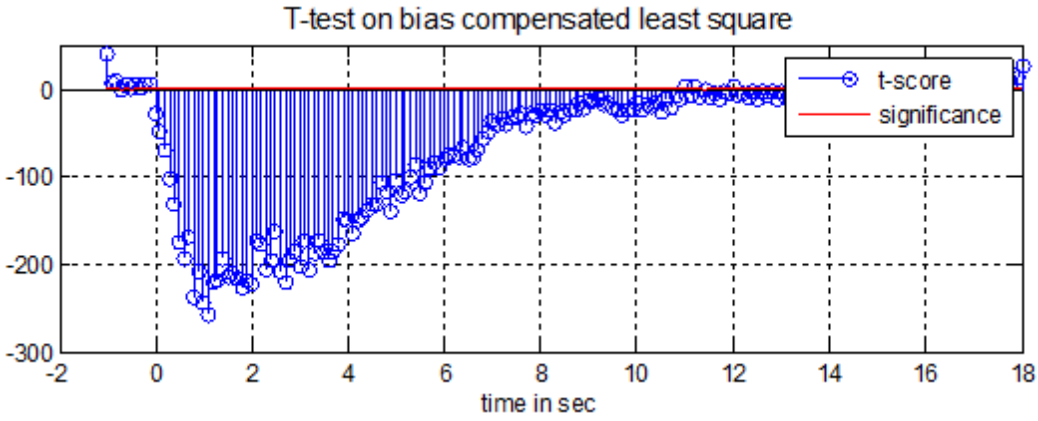

Figure 5-4: T-test on bias compensated least square estimate for a causal impulse response. T-test significant for t<0 sec even after bias removal

6. INVESTIGATING CAUSAL INFLUENCES USING GRANGER CAUSALITY

In task based studies, stimulus causes neural activity which subsequently causes change in oxygenation of hemoglobin. In other words in case of task-based paradigm, neural activity influences hemodynamic signal. However, as the activities during resting state are spontaneous it is possible that the hemodynamic signal may have some influence on neural activity. The method of granger causality is used to test for this affect.

6.1 METHOD

6.1.1 Granger causality

The basic idea behind granger causality is that if there are two time series X and Y (which are realizations of the corresponding random processes) then if X helps in the forecast or prediction of Y_t (the random process at time 't') i.e. reduces the prediction error of Y_t then X is said to granger-cause Y denoted as X => Y. More formally if we let $\overline{U_t}$= {X_{t-j}, Y_{t-j} for j=1, 2 …} i.e. the set containing all the past information about X and Y, $\overline{X_t}$ = {X_{t-j}| j=1, 2 …} i.e. the set containing the past information of X and $\overline{Y_t}$ = { Y_{t-j} , j=1, 2 …} i.e. the set containing the past information of Y, Y'_t denote the minimum mean square prediction (MMSE) of Y_t then if the MSE (Y'_t | $\overline{U_t}$) < MSE (Y'_t | $\overline{U_t} - \overline{X_t}$) then X is said to granger cause Y. Similarly if MSE (X'_t |$\overline{U_t}$) < MSE (X'_t | $\overline{U_t}$-$\overline{Y_t}$) then Y is said to granger cause X [10].

Suppose I have two discrete random processes X[t] and Y[t] and I want to study the relationship between them. Suppose that I model each of these processes by an autoregressive model of order p i.e. AR (p). Mathematically [9], [12]

$$X[t] = \sum_{j=1}^{p} a_{1j,t} X[t-j] + \epsilon_1[t] \tag{13}$$

$$Y[t] = \sum_{j=1}^{p} d_{1j,t} Y[t-j] + \eta_1[t] \tag{14}$$

Here the value of a random process at time 't' is predicted using only its own previous samples. $\epsilon_1[t]$ and $\eta_1[t]$ are the residuals or prediction errors with $\text{var}(\epsilon_1[t]) = \sigma^2_{\epsilon_1}$ and $\text{var}(\eta_1[t]) = \sigma^2_{\eta_1}$. Now suppose that I now model these two processes by a bivariate vector autoregressive model of order p (VAR (p)) in which in addition to using the past samples of a process itself, I also use the past samples of the other process i.e.

$$X[t] = \sum_{j=1}^{p} a_{2j,t} X[t-j] + \sum_{j=1}^{p} b_{2j,t} Y[t-j] + \epsilon_2[t] \tag{15}$$

$$Y[t] = \sum_{j=1}^{p} c_{2j,t} X[t-j] + \sum_{j=1}^{p} d_{2j,t} Y[t-j] + \eta_2[t] \tag{16}$$

Where $\epsilon_2[t]$ and $\eta_2[t]$ are the residuals or prediction errors with $\text{var}(\epsilon_2[t]) = \sigma^2_{\epsilon_2}$ and $\text{var}(\eta_2[t]) = \sigma^2_{\eta_2}$. The former model in which a process at time 't' is predicted using only its own previous samples is called the restricted model and the later model in which previous samples from both the processes are used is called the unrestricted model.

If X[t] and Y[t] are independent random processes then $\sigma^2_{\epsilon_2} = \sigma^2_{\epsilon_1}$ and $\sigma^2_{\eta_2} = \sigma^2_{\eta_1}$. To show this lets take an example. Suppose that Y[t] is originally an AR (1) process i.e.

$$Y[t] = a_1 Y[t-1] + w[t]$$

Here w[t] is taken to be white noise which is zero mean and var (w[t]) = σ_w^2. Y[t] will be wide sense stationary process with $R_{yy}(k) = \frac{\sigma_w^2 a_1^{|k|}}{1-a_1^2}$ and $\mu_y[t] = 0$. Now suppose that I form an MMSE estimate of Y[t] using a VAR (1) model i.e.

$$Y[t] = aY[t-1] + bX[t-1] + \eta_2[t]$$

The MMSE estimate is given

$$Rc = p$$

$$\begin{bmatrix} E(Y^2[t-1]) & E(Y[t-1]X[t-1]) \\ E(Y[t-1]X[t-1]) & E(X^2[t-1]) \end{bmatrix} \begin{bmatrix} a \\ b \end{bmatrix} = \begin{bmatrix} E(Y[t]Y[t-1]) \\ E(Y[t]X[t-1]) \end{bmatrix}$$

Since Y[t] is independent of X[t]

$$\begin{bmatrix} \frac{\sigma_w^2}{1-a_1^2} & 0 \\ 0 & R_{xx}(0) \end{bmatrix} \begin{bmatrix} a \\ b \end{bmatrix} = \begin{bmatrix} \frac{\sigma_w^2 a_1}{1-a_1^2} \\ 0 \end{bmatrix}$$

$$\begin{bmatrix} a \\ b \end{bmatrix} = \begin{bmatrix} \frac{1}{\frac{\sigma_w^2}{1-a_1^2}} & 0 \\ 0 & \frac{1}{R_{xx}(0)} \end{bmatrix} \begin{bmatrix} \frac{\sigma_w^2 a_1}{1-a_1^2} \\ 0 \end{bmatrix}$$

$$\begin{bmatrix} a \\ b \end{bmatrix} = \begin{bmatrix} a_1 \\ 0 \end{bmatrix}$$

Therefore $\eta_2[t] = Y[t] - aY[t-1] - bX[t-1] = w[t]$ and hence $\sigma_e^2 = \sigma_w^2$. On the contrary if Y[t] depends on X[t] then $\sigma_{\eta_2}^2 < \sigma_{\eta_1}^2$. and therefore whether X[t] has a causal influence on Y[t] can be quantified as

$$F_{X\to Y} = \ln\frac{\sigma_{\eta_1}^2}{\sigma_{\eta_2}^2}$$

Similarly the causal influence of Y[t] on X[t] can be quantified as $F_{Y\to X} = \ln\frac{\sigma_{\varepsilon_1}^2}{\sigma_{\varepsilon_2}^2}$. If X and Y are independent then $F_{X\to Y} = 0$ otherwise if X has causal influence on Y then $F_{X\to Y} > 0$. Similarly if $F_{Y\to X} = 0$ it implies that Y and X are independent and if $F_{Y\to X} > 0$ then Y has causal influence on X.

The process of determining causal influence is that given two time series X[t] and Y[t] we fit a VAR (p) model, find the MMSE coefficients of the model and find the variances of the residuals and determine the values of $F_{X\to Y}$ and $F_{Y\to X}$. In order to determine the order of the VAR (p) model, the Bayesian Information Criterion (BIC) is used $BIC\ (p) = \ln(\det(C)) + \frac{\ln(T)pn^2}{T}$ [10]. The order p for which BIC is minimum is chosen. Here 'T' is the total number of time points of X[t] and Y[t], 'p' is the number of parameters and 'n' is the total number of variables in the VAR model (X[t] and Y[t], 2 in our case). C is a covariance matrix

$$C = \begin{bmatrix} \sigma_{\epsilon_2}^2 & cov(\epsilon_2[t], \eta_2[t]) \\ cov(\epsilon_2[t], \eta_2[t]) & \sigma_{\eta_2}^2 \end{bmatrix}$$

The MMSE estimates of the coefficients in the VAR model can be approximated by the least-square estimates of the coefficients if the assumption of wide sense stationary and ergodic is made for the processes X[t] and Y[t]. But in this case even if the two time series X[t] and Y[t] are independent the variance of the residuals for the restricted and unrestricted models will not be equal. In fact since in the unrestricted model the past values of X[t] are being added therefore in the formulation of least squares they will create additional columns in the design matrix. Using more independent columns to span a vector in some higher dimensional space $\mathbf{R^n}$ will

always results in a smaller variance for the unrestricted model. So $F_{X\to Y}$ and $F_{Y\to X}$ will always be greater than zero even when the processes are independent. However, if the processes are independent then the extra columns will not cause a large decrease in variance and therefore $F_{X\to Y}$ and $F_{Y\to X}$ though positive will be small. Whereas in the case where there is some causal relationship they will be positive and large. In order to differentiate between the values for $F_{X\to Y}$ and $F_{Y\to X}$ which correspond to causal relationship it is a good idea to form a null distribution for the F-statistic. The null distribution will tell the probability of the F-statistic taking a particular value given that the processes are independent. The observed value F_{obs} can then be computed with a threshold F_t such that the $\Pr(F \geq F_t) = \alpha$ according to the null distribution. Here α is the significance level which is typically 5%. If the observed value $F_{obs} > F_t$ then it means that an event which has extremely low probability of happening (almost impossible) if the processes are independent has been observed which therefore could not have occurred by chance and hence we choose to reject the null hypothesis that the processes are independent and the large observed value F_{obs} indicates that there is causal relationship between X[t] and Y[t].

The null distribution was formed by calculating the least square estimate and finding $F_{X\to Y}$ and $F_{Y\to X}$ for a set of 500 pairs of independent observations of X[t] and Y[t]. The independent observations were obtained by performing a linear transformation of a random vector consisting of zero mean independent gaussian noise with variance 0.3. The linear transformation was performed in such a way so that the resulting X[t] observations have the same autocorrelation matrix as the LFP envelop and the resulting Y[t] observations have the same autocorrelation matrix as the optical signal. Mathematically,

$X[t]: LFP\ envelop, Y[t]: Optical\ signal$

$r_{xx}[k] = \lim_{N\to\infty} \frac{1}{N} \sum_{n=0}^{N} x[n]x[n+k]$ (Due to X[t] assumed wide sense stationary and ergodic)

$r_{yy}[k] = \lim_{N\to\infty} \frac{1}{N} \sum_{n=0}^{N} y[n]y[n+k]$(Due to Y[t] assumed wide sense stationary and ergodic)

$$R_{xx} = \begin{bmatrix} r_{xx}[0] & r_{xx}[1] & . & . & . & r_{xx}[+1000] \\ r_{xx}[-1] & r_{xx}[0] & r_{xx}[1] & . & . & r_{xx}[999] \\ . & r_{xx}[-1] & . & . & . & . \\ . & . & . & . & . & . \\ . & . & . & . & . & . \\ r_{xx}[-1000] & r_{xx}[-999] & . & . & . & r_{xx}[0] \end{bmatrix}$$

$$R_{yy} = \begin{bmatrix} r_{yy}[0] & r_{yy}[1] & . & . & . & r_{yy}[+1000] \\ r_{yy}[-1] & r_{yy}[0] & r_{yy}[1] & . & . & r_{yy}[999] \\ . & r_{yy}[-1] & . & . & . & . \\ . & . & . & . & . & . \\ . & . & . & . & . & . \\ r_{yy}[-1000] & r_{yy}[-999] & . & . & . & r_{yy}[0] \end{bmatrix}$$

Note that the autocorrelation values in the above matrices will be estimates since we only have finite amount of data.

Since R_{xx} and R_{yy} are symmetric matrices they can orthogonally decomposed as $R_{xx} = QDQ^T = Q\sqrt{D}I\sqrt{D}Q^T$. This decomposition shows that the transformation $X = A\vec{w} = Q\sqrt{D}\,\vec{w}$ where

$\vec{w} = [w_1\ w_2 \ldots w_{1000}]$ is a random vector containing independent zero mean gaussian random variables of variance 0.3. Applying this transformation on 500 independent realizations of $\vec{w}$ will give us 500 independent realizations of X of 1000 time points each which have the same autocorrelation structure as the actual LFP signal. In the same way, 500 independent realizations of Y of 1000 time points each can also be obtained which will have the autocorrelation of hemodynamic signal. Once we have these 500 pairs of realizations of X[t] and Y[t] in which

these two are independent of one another the coefficients of the restricted AR model and the unrestricted VAR model can be found using least squares criterion (BIC is used to obtain the value of p for each pair) and the values for $F_{X\to Y}$ and $F_{Y\to X}$ calculated. This will gives us a set of 500 values for the two statistics which serve as the null distribution for them. For the autoregressive restricted model (13) the least square formulation is

$$X[t] = \sum_{j=1}^{p} a_{1j,t} X[t-j] + \epsilon_1[t]$$

$$\begin{bmatrix} X[i1] \\ X[i1+1] \\ . \\ . \\ X[i2] \end{bmatrix} = \begin{bmatrix} X[i1-1] & X[i1-2] & . & . & . & X[i1-p] \\ X[i1] & X[i1-1] & . & . & . & X[i1+1-p] \\ . & . & . & . & . & . \\ . & . & . & . & . & . \\ X[i2] & X[i2-1] & . & . & . & X[i2-p] \end{bmatrix} \begin{bmatrix} a_{11} \\ a_{12} \\ \vdots \\ a_{1p} \end{bmatrix} + \begin{bmatrix} \epsilon_1[i1] \\ \epsilon_1[i1+1] \\ \vdots \\ \epsilon_1[i2] \end{bmatrix}$$

$$\boldsymbol{X} = A\vec{a} + \overrightarrow{\epsilon_1}$$

$$\boldsymbol{a}' = (A^T A)^{-1} A^T \boldsymbol{X}$$

And for the VAR unrestricted model (15) the least square formulation is

$$X[t] = \sum_{j=1}^{p} a_{2j,t} X[t-j] + \sum_{j=1}^{p} b_{2j,t} Y[t-j] + \epsilon_2[t]$$

$$\begin{bmatrix} X[i1] \\ X[i1+1] \\ . \\ . \\ X[i2] \end{bmatrix}$$

$$= \begin{bmatrix} X[i1-1] & X[i1-2] & . & . & . & X[i1-p] & Y[i1-1] & Y[i1-2] & . & . & . & Y[i1-p] \\ X[i1] & X[i1-1] & . & . & . & X[i1+1-p] & Y[i1] & Y[i1-1] & . & . & . & Y[i1+1-p] \\ . & . & . & . & . & . & . & . & . & . & . & . \\ . & . & . & . & . & . & . & . & . & . & . & . \\ X[i2] & X[i2-1] & . & . & . & X[i2-p] & Y[i2] & Y[i2-1] & . & . & . & Y[i2-p] \end{bmatrix}$$

$$\begin{bmatrix} a_{21} \\ a_{22} \\ . \\ . \\ a_2p \\ b_{21} \\ b_{22} \\ . \\ . \\ b_{2p} \end{bmatrix} + \begin{bmatrix} \epsilon_1[i1] \\ \epsilon_1[i1+1] \\ \vdots \\ \epsilon_1[i2] \end{bmatrix}$$

$$\boldsymbol{X} = [A\ B]\boldsymbol{c} + \boldsymbol{\epsilon_1} = D\boldsymbol{c} + \boldsymbol{\epsilon_1} \rightarrow \boldsymbol{c'} = (D^T D)^{-1} D^T \boldsymbol{X}$$

The above formulation will be applied to each of the 500 pairs of X[t] and Y[t]. Since X[t] is output in the above equations, the null distribution will be of $F_{Y\rightarrow X}$ statistic. Similarly using the model equations with Y[t] as output, the null distribution of $F_{X\rightarrow Y}$ statistic can also be obtained. Once the null distributions are found, the above formulation can be used on the original LFP and optical signal (whose time autocorrelation was used in obtaining the null distributions) to obtain the observed values of $F_{X\rightarrow Y,obs}$ and $F_{Y\rightarrow X,obs}$. Then the probability of the statistic being greater than the observed values under the null distribution is found by counting the values of F which are greater than the observed values and dividing by the total number of values (500 in our case).

6.1.2 Validating the granger causality approach

Recall that the method of granger causality is based on the fact that given two time series X and Y, if the inclusion of previous samples of Y in the vector autoregressive model improves the prediction of X then Y is said to granger-cause X. Granger causality has been used in neuroscience and fMRI research to show that causal relationships exist between physiological parameters such as local field potential (LFP), cerebral blood flow (CBF) etc [12]. But these signal measurements will always be inherently noisy. As we have seen, the presence of noisy affects the causality of least-square estimate of HRF therefore it would also be interesting and

important to look into whether the presence of noise can result in false granger-causal relationships. Given two noisy time-series X and Y where X is independent of Y and only depends on its own previous samples can we still get a value of F-statistic significant to show that Y granger-causes X? Simulations are used to look into this question.

(1) Simulation

Suppose that X[n] is an AR (2) process and Y[n] is related to X[n] in the following way

$$X[n] = 0.9X[n-1] - 0.5X[n-2] + e_1[n]$$

$$Y[n] = 0.8Y[n-1] - 0.5Y[n-2] + 0.16X[n-1] + 0.5X[n-3] + e_2[t]$$

Here $e_1[n]$ and $e_2[n]$ are zero mean i.i.d gaussian noise with variance 0.3.

An autoregressive model and a vector autoregressive model (VAR) of order 3 for X[n] would be

$$X[n] = \sum_{j=1}^{3} a_{2j,t} X[n-j] + \epsilon_1[n] \tag{17}$$

$$X[n] = \sum_{j=1}^{3} a_{2j,t} X[n-j] + \sum_{j=1}^{3} b_{2j,t} Y[n-j] + \epsilon_2[n] \tag{18}$$

$\epsilon_1[t]$ and $\epsilon_2[t]$ are residuals. Since X is originally an AR(2) process then the MMSE estimates for the AR model above would provide the minimum error. Moreover, since X[n] does not depend on Y[n] and its previous samples and since the VAR model already includes the AR model (in form of previous samples of X) , we expect the MMSE estimates for the $b_{2j,t}$ coefficients to be zero and the variance of residual $\epsilon_2[t]$ to be the same as $\epsilon_1[t]$ (Recall that we talk about the MMSE estimates despite the fact that we actually find least square estimates of the coefficients in the above model because under assumption of wide-sense stationary and ergodic

for X[n] and Y[n], least square estimates are an asymptotically unbiased estimate of the MMSE estimate). So 500 realizations of X[n] and Y[n] of length 1000 are generated according to eq. (17) and (18). Then for each pair of realization a null distribution for the $F_{X\to Y}$ and $F_{Y\to X}$ statistic (causal influence of X on Y and causal influence of Y on X) is generated. Then coefficients for the AR and VAR model are estimated as per the least-square criterion, observed values for $F_{X\to Y}$ and $F_{Y\to X}$ are calculated and compared against a threshold corresponding to 5% significance level $F_{X\to Y,threshold}$ and $F_{Y\to X,threshold}$. If $F_{obs} > F_{threhold}$ then the corresponding causal relationship is statistically significant. We expect $F_{X\to Y}$ to be statistically significant and $F_{Y\to X}$ to be statistically insignificant since Y[n] depends on previous values of X[n] but X[n] does not depend on previous values of Y[n]. This same procedure is repeated after corrupting X[n] and Y[n] by i.i.d zero mean gaussian noise to investigate what difference the presence of noise creates.

6.2 RESULTS AND DISCUSSION

The method described in section 6.1.1 of obtaining null distributions for the F-statistic and then computing the coefficients for the models using least-squares criterion was performed for each of the subjects. The null distributions obtained for different subjects were also different since the different LFP envelop and optical signals for each subject would have different time autocorrelation. Figure 6.1a and 6.1 b shows the null distribution (histograms) of $F_{X\to Y}$ and $F_{Y\to X}$ statistic respectively for one of the subjects. As is expected the histograms peak at values close to zero since the underlying X[t] and Y[t] observations are independent.

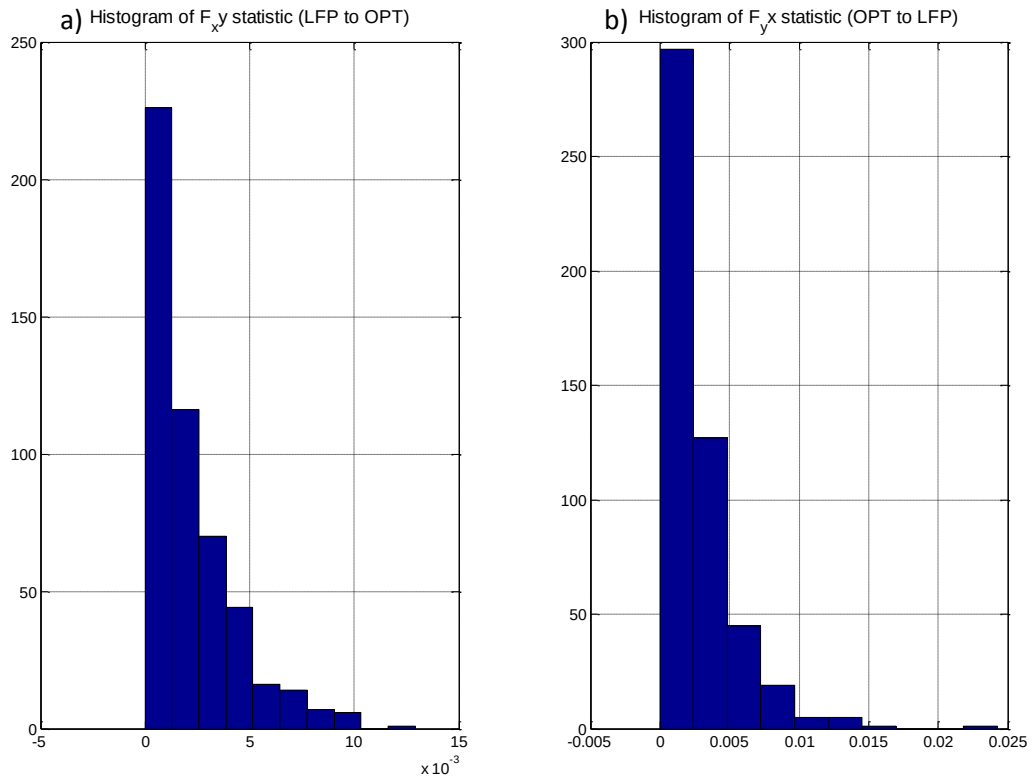

Figure 6-1: a) Histograms of Fxy (causal influence from LFP envelop to optical signal) and b) Fyx (causal influence from OPT to LFP signal) using independent observations

.

Figure 6.2 shows the observed values of $F_{X\to Y}$ indicating causal influence from LFP envelop to hemodynamic signal (blue bar) and $F_{Y\to X}$ indicating causal from hemodynamic signal to LFP envelop (red bar) for different subjects (subject nos. on x-axis). On the graph the blue line with green square makers indicates the $F_{X\to Y,threshold}$ corresponding to 5% significance level. And the red line with red circle makers indicates the $F_{Y\to X,threshold}$. The observed values of $F_{X\to Y}$ exceed the threshold for all subjects indicating that the LFP envelop granger causes hemodynamic signal. Also the observed values of $F_{Y\to X}$ also exceed the threshold (for 5% significance level) except for one subject. From this we conclude that the hemodynamic signal also granger causes the neural activity.

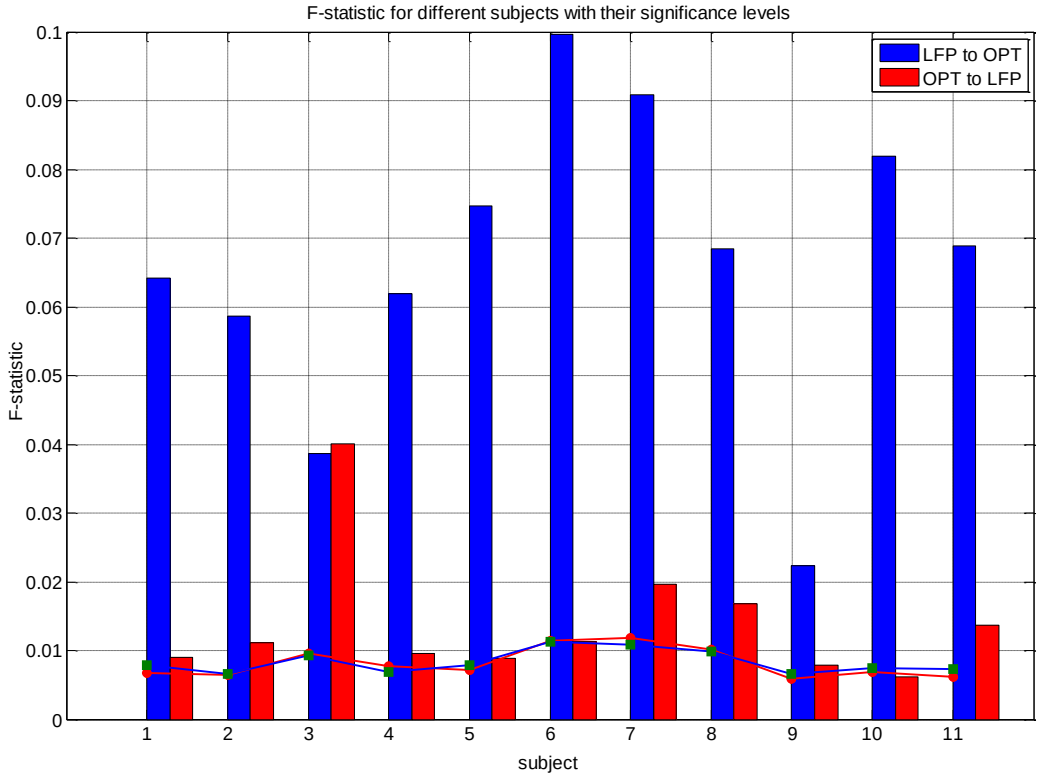

Figure 6-2: Blue bars show the observed values for Fxy and the red bars show the observed values for Fyx. The blue line with green square markers represents the threshold value of Fxy at 5% significance level from the null distribution. The red lines with red circle markers represent the threshold value of Fyx at 5% significance level from the null distribution.

Figure 6.3 shows the statistic $F_{X\to Y}$ calculated from noise-free and noisy X[n] and Y[n] simulated using the example model. Only 10 of the 500 simulated realizations were used. The blue bar shows $F_{X\to Y}$ without noise. The blue line indicates the corresponding $F_{X\to Y,threshold}$ for 5% significance level obtained by generating a null distribution as described in the chapter on granger causality. As expected the $F_{X\to Y,obs} < F_{X\to Y,threhold}$ i.e. statistically insignificant for all cases since in the example model X[n] does not depend on Y[n]. However, the presence of noise in input causes $F_{X\to Y,obs} > F_{X\to Y,threhold}$ as indicated by the red bar and the corresponding $F_{X\to Y,threshold}$ indicated by the red line. This shows that the presence of noise can

lead to false causal relationships e.g. for the example model in which X[n] does not depend on Y[n] at all, the below graph indicates that Y[n] granger causes X[n].

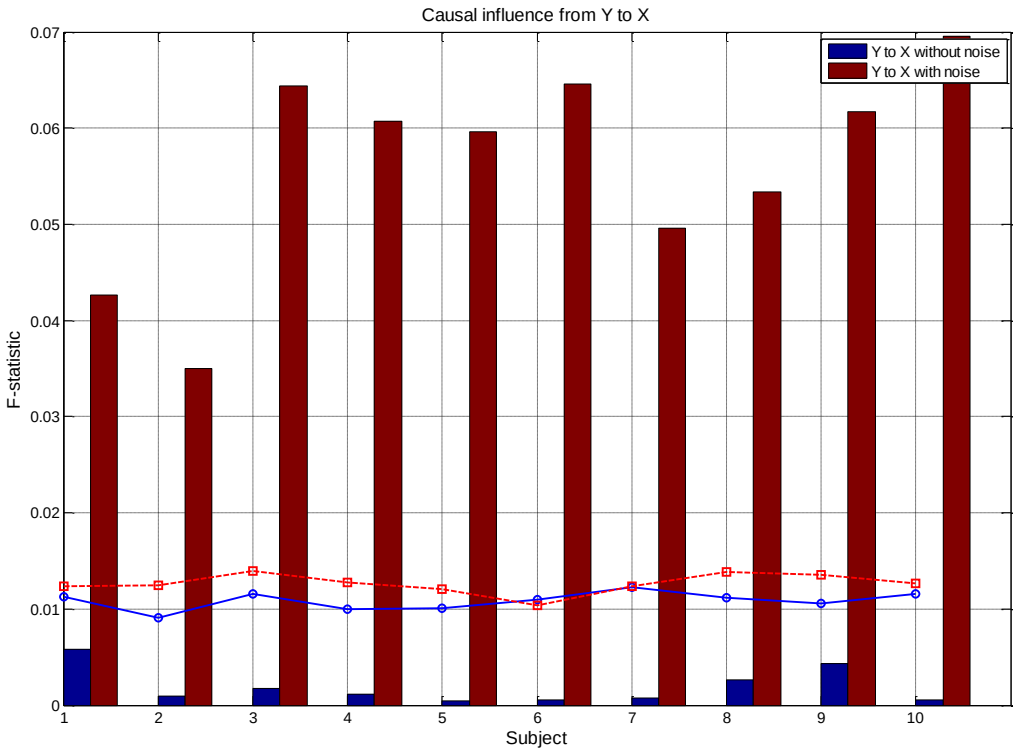

Figure 6-3: This figure shows the causal influence of Y on X for the example model considered above. The blue bar and blue line indicates the F-statistic (y to x) and the F-threshold respectively when there is no noise. The red bar and red line shows the F-statistic (y to x) and F-threshold in presence of noise.

7. DISCUSSION AND CONCLUSIONS

In this study we investigated the linearity of relationship between neural activity and hemodynamic signal, the causal influences between the two signals and the causality of the hemodynamic response function during resting state in rat brain. Two approaches were used to investigate linearity. One approach utilized the superposition principle in which the predicted response due to group of bursts, obtained by convolving the group of bursts with an estimated hemodynamic response function, was compared with the actual response. It was found that contrary to results reported for task-based studies, the predicted response did not consistently over or under estimated the actual response and hence there was no evidence of non-linearity. From this it was concluded that during resting state the system between neural activity and hemodynamic signal can be modeled well by an LTI system. The approach of sliding window RLS was also used to investigate whether the impulse response chances with input parameter such as burst-width and it was found using t-test that the obtained correlations were not statistically significant which again corroborates our conclusion about LTI system being a good model for resting state. The significance of this finding is that it allows us to make confident interpretation of neural activity from BOLD in situations where the subject is anaesthetized up to the level used in [6] which results in burst-suppression activity. However, it is still unclear whether the same results will hold in rats under lighter anesthesia because the neural activity will be much more and different from burst suppression activity. Also it is unclear as to whether the above results will hold for humans because in awake humans during resting state the neural activity is much rich and not high for some time and zero for other i.e. burst-suppression. Rather the neural activity is continuous. Hence future work is needed to verify whether these conclusions hold for humans and under different level of anesthesia.

The spontaneous nature of neural activity and hemodynamic signal during resting state and the presence of vasomotion allows for the possibility of a third common mechanism deriving these activities and hemodynamic signal having some causal influence on neural activity. The approaches of least-square filtering and granger causality were used to investigate these possibilities. Moreover, signal such as LFP and BOLD and other measured biological signals always have some inherent noise. For example the LFP envelop used as input in this study is itself a noisy estimate of the true neural activity. Therefore we also studied the effect of noise on causality of HRF and on granger causal influences. It was shown that the HRF turn out to non-causal and that the non-causality in statistically significant. However, it was also found that the presence of noise in signals makes filter estimates obtained via popularly used methods such as least-square and weiner filtering biased. The estimated impulse responses are blurred since they are convolved with a two sided distortion sequence in time. The consequences of this finding for fMRI studies are that the Hemodynamic Response Functions (HRF) estimates, obtained using these techniques, do not represent the true underlying physiological system. Hence inferring the system from HRF requires caution. Furthermore, it was shown that the presence of noise leads to false granger causal influences between signals raising questions on the results revealed by previous studies [12] and stressing the need of practicing caution while interpreting results. The presence of noise can also make impulse response estimates non-causal therefore our finding that HRFs during resting state turn out to be statistically non-causal does hint towards the possibility of a third common mechanism such as vasomotion controlling both neural activity and oxygenation during resting state however, it is not conclusive and further work is needed to exactly eliminate the effect of noise.

8. REFERENCES

1. Zhang, N., X.-H. Zhu, and W. Chen, Investigating the source of BOLD nonlinearity in human visual cortex in response to paired visual stimuli. Neuroimage, 2008. **43**(2): p. 204-212.
2. Berens, P., N.K. Logothetis, and A.S. Tolias, Local field potentials, BOLD and spiking activity–relationships and physiological mechanisms. Nat. Precedings, 2010.
3. Liu, H.-L. and J.-H. Gao, An investigation of the impulse functions for the nonlinear BOLD response in functional MRI. Magnetic resonance imaging, 2000. **18**(8): p. 931-938.
4. Fox, M.D. and M.E. Raichle, Spontaneous fluctuations in brain activity observed with functional magnetic resonance imaging. Nature Reviews Neuroscience, 2007. **8**(9): p. 700-711.
5. Jia, L.-J., et al. On bias compensated least squares method for noisy input-output system identification. in Decision and Control, 2001. Proceedings of the 40th IEEE Conference on. 2001. IEEE.
6. Pan, W.J. and S. keilholz, Fiber optical hemodynamic recording in deep brain areas in rats Organization of Human Brain Mapping, 2015.
7. Rombouts, S.A., et al., Altered resting state networks in mild cognitive impairment and mild Alzheimer's disease: an fMRI study. Human brain mapping, 2005. **26**(4): p. 231-239.
8. Zhang, N., et al., Noninvasive study of neurovascular coupling during graded neuronal suppression. Journal of Cerebral Blood Flow & Metabolism, 2008. **28**(2): p. 280-290.
9. Ding, M., Y. Chen, and S. Bressler, Granger causality: basic theory and application to neuroscience. 2006. arXiv preprint q-bio/0608035.
10. Helmut, L., Introduction to multiple time series analysis. 1993, Berlin: Springer.
11. Uludag, K., D.J. Dubowitz, and R.B. Buxton, Basic principles of functional MRI. Clinical MRI. Elsevier, San Diego, 2005: p. 249-287.
12. Huang, L., et al., Hemodynamic and electrophysiological spontaneous low-frequency oscillations in the cortex: directional influences revealed by Granger causality. Neuroimage, 2014. **85**: p. 810-822.
13. Hayes, M.H., Statistical digital signal processing and modeling. 2009: John Wiley & Sons.
14. Moon, T.K.S. and C. Wynn, Mathematical methods and algorithms for signal processing. 2000.
15. Sheline, Y.I., et al., *The default mode network and self-referential processes in depression.* Proceedings of the National Academy of Sciences, 2009. **106**(6): p. 1942-1947.
16. Goutte, C., F.Å. Nielsen, and L.K. Hansen, *Modeling the hemodynamic response in fMRI using smooth FIR filters.* Medical Imaging, IEEE Transactions on, 2000. **19**(12): p. 1188-1201
17. Hansen, M.H. and B. Yu, *Model selection and the principle of minimum description length.* Journal of the American Statistical Association, 2001. **96**(454): p. 746-774.

18. MORITA- TSUZUKI, Y., E. Bouskela, and J. Hardebo, *Vasomotion in the rat cerebral microcirculation recorded by laser- Doppler flowmetry.* Acta physiologica scandinavica, 1992. **146**(4): p. 431-439.